Reply to reviewers

acp-2014-970

Chemical characterization of submicron regional background aerosols in the Western Mediterranean using an Aerosol Chemical Speciation Monitor

The authors would like to thank the reviewers for their comments and suggestions, which helped improving the quality of this work. A new version of the manuscript has been prepared following the suggestions from the reviewers. We provide below detailed replies to each of the comments in a point-by-point manner.

Reviewer#1. The manuscript of Minguillón et al. represents the results obtained by using an Aerosol Chemical Speciation Monitor over a one-year period in a regional background station of the Western Mediterranean (Montseny, Spain). The mass concentrations of submicron organics, sulphate, ammonium, nitrate and chloride obtained by the ACSM are compared to concurrent off-line PM1 chemical (for inorganics) and thermal-optical (for organic carbon) analysis of filters. The sum of the ACSM components, using a time-dependent collection efficiency instead of the widely used constant 0.5, together with black carbon correlated well with PM1 concentrations determined by an optical particle counter. Nevertheless discrepancies were observed, mainly for organics, which was attributed to an underestimation of the relative ionization efficiency of the organic aerosol (OA). The importance of these discrepancies become more important if one considers the fact that the OA was found to be the major constituent of the submicron aerosol throughout the year. The source apportionment of the OA, using the ME-2 toolkit within the Positive Matrix Factorization analysis environment, revealed three major sources both during summertime and during wintertime, as well. During summer the main OA identified were hydrocarbon-like OA (HOA), and two oxygenated OA; one semi-volatile (SV-OOA) and one of low volatility (LV-OOA). During winter again an HOA was identified, together with a biomass burning OA (BBOA) and oxygenated OA (OOA), while the two different OOA components that were identified during summer could not be resolved. Finally, focusing on an intense wildfire episode close to the measurement site, a BBOA profile was identified, which was found to be very similar to BBOA profiles formerly identified in former studies at the same site, establishing a region-specific BBOA_MSY mass spectrum.

The paper is well written and easy to follow, though there are several details missing and more thorough discussion should be made in specific sections. Other than that the paper can be recommended for publication after addressing the issues listed below.

Reviewer#1. Specific comment 1) One of the main features of the manuscript that the authors draw our attention to is the comparison of the ACSM data with collocated off-line PM1 measurements and with total PM1 measured by an optical particle counter. Nevertheless it is clearly stated that the OPC is corrected with the simultaneous 24h gravimetric measurements, but there is no mentioning of why the gravimetric measurements are believed to be the reference. Quartz filters are known to absorb water and volatile organics, depending on the sampling protocol (preheated filters or not). I assume that, as no preheating of the filters is mentioned, there was none, but still, with the high RHs that can be seen in Figure S2, how is it guaranteed that the filters do not contain significant amounts of humidity from the sampling? Apart from the Quartz filters, are there also any Teflon filters, which are not expected to absorb neither water nor volatiles, collected in order to compare? Furthermore, I would expect a significant daily variability in the 30-min ACSM measurements that, for sure, cannot be captured in the 24h filters. Therefore, how is this correction made? Finally, in Cusack et al. (2013) it is mentioned that a Scanning Mobility Particle Sizer (SMPS) is also located in the Montseny Station; were the PM1 concentrations (ACSM+BC) compared to the mass estimated using the SMPS volume?

Reply to Reviewer#1. Specific comment 1)

The authors acknowledge the limitations of the gravimetric determination of total PM_1, and are aware of the possible artifacts. It should be noted that the PM_1 high-volume sampler is located in a container with controlled temperature (as explained in the methods section), which reduces the negative artifacts due to volatilization of some components (mainly organic matter) at high temperatures that could occur in summer. Regarding the quartz filters treatment: the filters were pre-treated at 220°C during four hours before sampling, and filters were stabilized at controlled T and RH (20°C and 50% relative humidity) before weighing before and after sampling, according to EN12341 standard. Therefore, it is true that the filters can contain some water, not eliminated during the stabilization period, but it is expected to be a low proportion of the total mass. In any case, the authors consider that it is better to correct the OPC data with the gravimetric measurements than not correcting it at all, and they follow the guidelines for data treatment obtained from real-time PM_x determination (Alastuey et al., 2011, "PM_{10} measurement methods and correction factors: 2009 status report", http://acm.eionet.europa.eu/docs/ETCACM_TP_2011_21_PM10Equivalence.pdf). In this report it is stated that measurements from real-time monitors should be compared with simultaneous gravimetric measurements and corrections should be applied. The correction is made as follows: real-time PM_1 concentrations from OPC are daily averaged and compared to 24-h gravimetric PM_1 concentrations. The parameters resulting from this comparison are then used to correct the hourly PM_1 data from the OPC.

The text in the revised manuscript has been modified to include the details on filter stabilization, and to include the reference where the correction of real-time measurements method is explained:

"Gravimetric PM_1 determination was carried out by weighing the filters before and after sampling, after stabilization in a conditioned room (20°C and 50% relative humidity)."

"PM_1 hourly concentrations were measured using an optical particle counter (GRIMM, model 180) and corrected with the simultaneous 24-h gravimetric measurements (Alastuey et al., 2011)"

Unfortunately, there are no Teflon filters available for the sampling period.

The PM_1 concentrations calculated from ACSMcomponents+BC were compared to the mass estimated using the SMPS volume for 2012 period (given that SMPS data were not available for 2013), resulting in a slope close to unity with a squared Pearson correlation coefficient of 0.77. This information has been added in the revised version of the manuscript in the methods and the results section. Moreover, the figure below has been added in the supplementary material as Figure S4.

Methods: "Particle number size distributions (9-820 nm) were measured by a Scanning Mobility Particle Sizer (SMPS), comprising a DMA connected to a CPC (TSI 3772), with a system designed and manufactured at the Leibniz Institute for Tropospheric Research (Wiedensohler et al., 2012). The mass concentration from SMPS data was calculated from the total volume of particles and the composition-dependent density calculated basedon the ACSM chemical composition."

Results: "The sum of ACSM components and BC concentrations was also compared to the mass concentration calculated from SMPS data, resulting in a strong correlation (squared Pearson correlation coefficient, R^2=0.77) and a slope very close to unity (0.997) (Figure S4)."

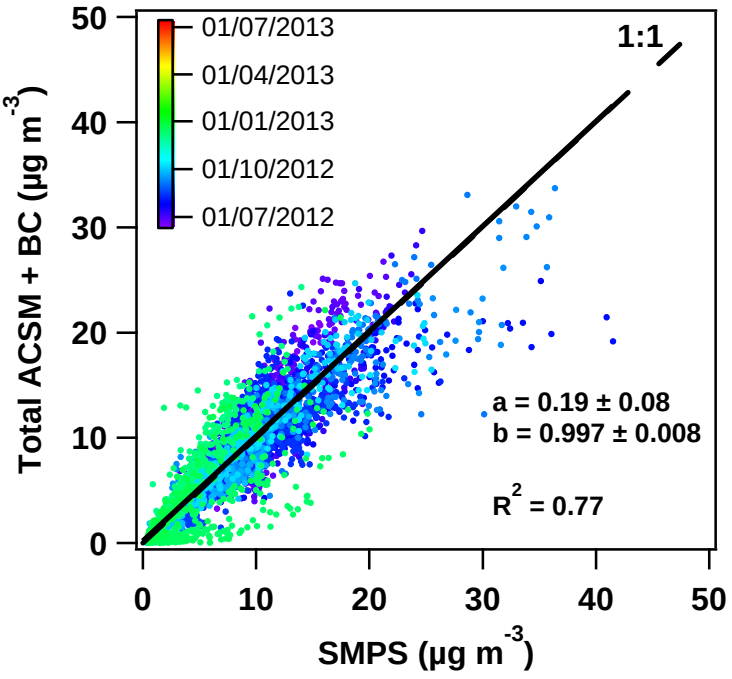

Figure S4. ACSM components + BC concentrations vs mass concentration calculated from Scanning Mobility Particle Sizer (SMPS) data coloured by the sampling time (dd/mm/aaaa). Data availability for SMPS data covered only 2012 period. Line and parameters correspond to least orthogonal distance fit (y=a+bx). The wild fire period is excluded from the fit.

Reviewer#1. Specific comment 2) It is mentioned in the manuscript that instead of a constant, collection efficiency (CE) of 0.5, a time-dependent CE is used, following the approach of Middlebrook et al. (2012). In the cited paper, an algorithm is developed in order to calculate composition-dependent CE values, in order to account for acidic sulfate particles, aerosol containing a high mass fraction of ammonium nitrate and high organic fraction from biomass burning emissions. In the current manuscript there is no mention of the aerosol acidity, biomass burning emissions appear to be limited and also nitrate concentrations seem to have a maximum contribution (around 20%) during winter. It would be helpful if the authors provided, even in the supplementary material, a figure that shows if and how much the used time-dependent CE deviated from the constant 0.5, especially if there is a seasonal variability observed.

Reply to Reviewer#1. Specific comment 2)

A short explanation of how much the CE differs from the default 0.45 value is included in the revised manuscript, as well as a figure with the CE time series in the supplementary material:

"The time-dependent CE equalled the default value of 0.45 for most of the period, and increased up to 0.65 during the colder period (Figure S3)."

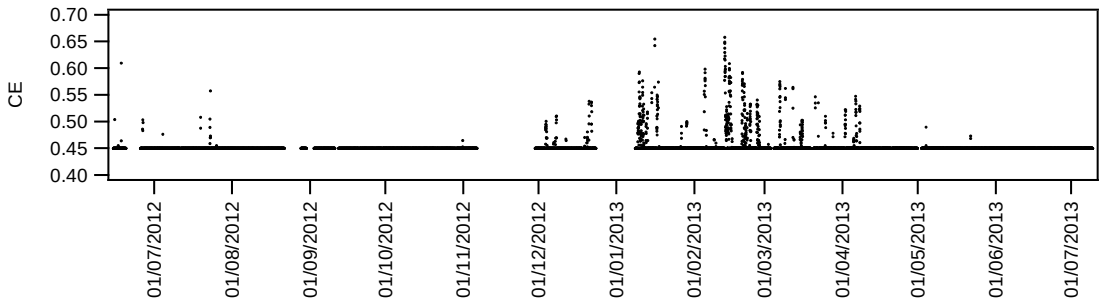

Figure S3. Time-dependent CE calculated with the Middlebrook approach (Middlebrook et al., 2012).

Reviewer#1. Specific comment 3) The claim that the second identified factor by the PMF analysis, during the wildfire episode, is and Aged BBOA, clearly needs a better reasoning and a more thorough discussion. The mass spectrum is very similar with common OOA found in the literature and no correlations are given with external tracers, such as black carbon, to support this assumption. Furthermore, why should that OOA factor have only one source origin and not be, partially, a pre-existing, background OOA that, clearly from the time series, may be also the end product of atmospheric transformation of BBOA, as well? What do their diurnal variability look like, is it similar? My greatest concern is the nomenclature, solely stating it as "Aged BBOA".

Reply to Reviewer#1. Specific comment 3)

The main goal of the source apportionment of OA carried out for the period of this event was to clearly differentiate the fresh BBOA contribution, from aged or background OA. Hence, different tests were carried out until reaching a satisfactory solution with two factors, one of them clearly identified as BBOA. Given the high impact of the wildfire event on the ambient

submicron aerosol concentrations, the authors made the assumption that the rest of the contributors to ambient concentrations during the wildfire event were close to negligible. This fact, together with the time series of the second OA factor identified for this episode (tracking partially that of BBOA factor), led the authors to name this factor as Aged BBOA. Nevertheless, the authors agree that the source profile resembles that of typical OOA factors and that a contribution from other OOA may also take place during the episode. Therefore, the name of the factor has been changed to simply OOAm (where the m stands for mix). The discussion on the wildfire event has been modified accordingly as follows:

"In order to investigate the wildfire source, an unconstrained source apportionment (PMF) of the organic aerosol fraction during this episode was carried out. The PMF resulted in two factors, one representing the fresh biomass burning organic aerosol (named as BBOA_MSY) and another one interpreted as the mix of other OA sources and aged BBOA, named as OOAm (where the m stands for mix). The interpretation of the factors is based on their mass spectral source profiles and the time series of their contributions. The BBOA_MSY shows higher peaks for the specific tracers of biomass burning (*m/z* 60 and *m/z* 73) (Alfarra et al., 2007) than the OOAm, which indicates that the primary BBOA is well represented by this factor. Moreover, the f44 (ratio of *m/z* 44 (mostly CO_2^+) to total signal in the component mass spectra), an indicator of oxygenated organic species (Alfarra et al., 2007), was higher for the OOAm than for the BBOA_MSY factor, which indicates that this factor corresponds to a more oxidized aerosol. On the other hand, the f43 is higher than the f44 in the BBOA_MSY factor, whereas it is the other way around (f44 much higher than f43) in the OOAm. These differences in relative intensities indicate the differences in the age of the aerosol (Ng et al., 2010) and further lead to differentiate the factors as fresh BBOA and OOAm. The SOA formation from biomass burning has been reported to be quick (Heringa et al., 2011), and hence part of the OOAm factor is formed of aged BBOA, which also explains that the time series of the OOAm factor partially tracks that of the BBOA_MSY. The BBOA_MSY profile found here is very similar to a BBOA profile found for Montseny in March 2009 (Minguillón et al., 2011) (https://sites.google.com/site/amsglobaldatabase) and to an average profile for BBOA from various datasets (Ng et al., 2011a) (Figure S9). The f60 in the BBOA_MSY factor is 0.014, similar to the f60 in these other two BBOA profiles (0.017 and 0.024). It has been also compared to the BBOA found in the background of Paris (Crippa et al., 2013), with which some more differences were found, mainly our profile has higher *m/z* 43 and *m/z* 41 signals and lower *m/z* 60 (Figure S9). This BBOA_MSY mass spectrum is considered specific for the study area and hence it can be later used for other studies in the region, to be fed to the ME-2 model in order to quantify the BBOA contribution. We have done so in the present study for the winter period. Whereas the time series of both factors were similar, the BBOA_MSY contribution showed more intense peaks, and the increase in the OOAm was slightly higher for the second part of the main peak on the 23 July."

<u>Reviewer#1. Specific comment 4)</u> I would have expected, even in the supplementary material, a more thorough discussion on the selected PMF solutions; stability of the solution, residuals, correlations with external tracers, possibly a more detailed comparison with external mass spectra (e.g. squared Pearson coefficients).

Reply to Reviewer#1. Specific comment 4)

The variation of atmospheric aerosols in the regional background is usually driven by the transport of pollutants from nearby polluted areas, with little influence from local sources, and some influence from local atmospheric processes. Montseny site is not an exception and therefore several aerosol components show the same variation. For instance, whereas the diurnal variation of HOA in a city is usually characterized by the two rush hour peaks and nicely correlates with BC, the HOA found at Montseny is the result of the transport from the polluted areas, and therefore the diurnal pattern is characterized by a single increase around midday, as it happens with the rest of pollutants. This is a drawback to use the correlations among different pollutants with the aim of confirming their common origin. This is the case for the different organic sources found at Montseny. Nevertheless, the authors did study the correlations between the OA sources time series with external tracers, but results were interpreted with caution bearing in mind the characteristics described above. This is the reason for not giving too much relevance to these correlations in the manuscript. However the authors understand the need for a more thorough discussion of the selected PMF solutions and it has been included in the revised manuscript, as well as an additional figure in the supplementary material.

The text in the revised manuscript is now as follows:

"The application of ME-2 to the warmer period resulted in a solution with 3 factors: a hydrocarbon-like OA (HOA), a semi-volatile oxygenated OA (SV-OOA) and a low-volatile oxygenated OA (LV-OOA). This solution was chosen based on several tests with different number of factors and different a-values for the constrained factors, taking into account the correlations with external data, the diurnal patterns and the residuals, following the strategy described by Crippa et al. (2014) and Canonaco et al. (2013). The HOA factor was constrained using an average HOA factor (HOA_avg) from different datasets (Ng et al., 2011a). An a-value range from 0.05 to 0.3 was explored and an a-value of 0.2 was finally selected, which was a compromise between a higher Squared Pearson correlation coefficient between HOA and BC (which increased when increasing the a-value) and the physically meaningful profiles of the whole solution (i.e. assessing the profiles of the LV-OOA and SV-OOA factors). BC concentrations correlated moderately with HOA (squared Pearson coefficient R^2= 0.51). The SV-OOA shows higher 43-to-44 ratio compared to the LV-OOA, together with a lower f44, which are the main differences between these two profiles (Figure 8a). The BBOA contribution in summer is expected to be low based on previous studies carried out in July 2009 (Minguillón et al., 2011) and on the low f60 registered in the present study in summer (Figure S10), which is below the background threshold (0.003) established by Cubison et al. (2011). Hence, the BBOA factor was not identified and it was not constrained by the ME-2 in summer.

During the warmer period, the HOA accounted for 13% (0.7 μg m^{-3}), whereas the LV-OOA and the SV-OOA accounted for 45% and 42% of the total OA (2.4 μg m^{-3} and 2.2 μg m^{-3}), respectively (Figure 8c). As explained before, the location and meteorological conditions at MSY result in an increase of pollutants concentrations starting at mid-morning, caused by the breeze transport from populated areas to the regional site. This variation is clearly observed for BC (Figure 9), which showed a moderate correlation with HOA (R^2= 0.51). Nevertheless, the

midday increase in the concentration of SV-OOA is larger than that of BC, and therefore it cannot be only explained by the transport of pollutants, including the SOA formed during the transport, but it is attributed to the formation of SOA during these hours in MSY. Hence, the SOA formation can be estimated as the additional increase with respect to that of BC (considered in % of the average concentration during the night hours), which results in a local SOA formation of 1.1 μg m^{-3}. This SOA may result mainly from biogenic precursors, in agreement with the 70% of non-fossil SOA found in March 2009 (Minguillón et al., 2011). The flatter diurnal pattern of LV-OOA (Figure 9) points to a more regional and well-oxidized aerosol, which could be interpreted as the regional background SOA. This SOA formation during warm periods was also observed by Cusack et al. (2013), who studied nucleation and particle growth events, identifying both of them even under polluted conditions at MSY.

In the colder period, the application of ME-2 resulted in a solution with 3 factors: hydrocarbon-like OA (HOA), biomass burning OA (BBOA) and oxygenated OA (OOA) (Figure 8b). A solution with two OOA factors was investigated and it was not meaningfully interpretable. Probably the small temperature range variation in winter results in not enough diurnal variation in f43 and f44 for a split of the OOA in SV-OOA and LV-OOA. As per the warmer period, the final solution was chosen based on the strategy described by Crippa et al. (2014) and Canonaco et al. (2013). The residuals for the chosen solution did not show any daily pattern or *m/z*-dependent pattern, which is a good indicator that the selected solution explains the OA variation. For coherence with the warmer period, the HOA factor was based in an average HOA factor (HOA_avg) from different datasets (Ng et al., 2011a), and it was constrained with an a-value of 0.1. This a-value was chosen based on the correlation between the HOA contribution and the BC concentrations found for different a-values tests. The HOA contribution shows a relatively strong correlation with BC concentrations (squared Pearson coefficient R^2=0.70). The HOA spectral profiles found for summer and winter are quite similar, and hence the HOA contributions in summer and winter can be compared directly. The BBOA factor was decided to be constrained based on the f60 signal, which was above the aforementioned threshold of 0.003 (Figure S10). It was based in the BBOA_MSY profile found for the wildfire episode that took place during this study, constrained with an a-value of 0.1. The a-value was chosen with the following criteria: preference for a low a-value given that the anchor profile used was site-specific, residuals for the *m/z* 60 not showing any diurnal pattern, contribution of the BBOA factor to the total *m/z* 60 (which reached 64% for the chosen solution). The resulting BBOA profile has a higher *m/z* 44 signal than the BBOA_MSY, which may indicate differences in the biomass burning emissions from the wildfire event compared to the emissions from regular biomass burning, or it could indicate that the BBOA contribution identified here may be partially mixed with some oxidized OA. The single winter OOA factor identified shows higher f44 than both LV-OOA and SV-OOA in summer. This higher degree of oxidation of the OA in winter indicates that there is less newly-formed SOA during winter compared to summer. A similar variation was observed in Zurich (Canonaco et al., 2014). The OOA contribution correlates moderately with sulphate (R^2=0.49), relatively strongly with nitrate (R^2=0.73) and more strongly with ammonium (R^2=0.79).

The major OA constituent in winter was the OOA, with 59% (1.5 μg m^{-3}), whereas the HOA and BBOA accounted for 12% (0.3 μg m^{-3}) and 29% (0.7 μg m^{-3}) of the total OA, respectively (Figure 8d). Note that the BBOA contribution may be mixed with some OOA as stated before, given

the relatively high signal at *m/z* 44 and hence the pure BBOA contribution would be lower than that determined. Actually it accounts for 6% of the total signal at *m/z* 44. Nevertheless, strong correlation (R^2=0.77) was found between the BBOA contribution and the potassium concentrations determined in 24-h PM_1 samples (Figure S11), which further confirms the existence of this source at MSY in winter. The relative BBOA contributions found in the present study are similar to those found in a previous study in March 2009 using a HR-ToF-AMS, where the HOA represented 7% of the total OA, the BBOA contributed with 9% and the rest was attributed to OOA (Minguillón et al., 2011;Crippa et al., 2014). The discrepancy in the BBOA contribution (29% vs 9%) may be due to the different sampling periods (the current study included Nov 2012-March 2013 whereas the previous study only included March 2009), to the mixture of some OOA in the BBOA factor for the present study, and/or to the possible increase of biomass burning due to the climate and energy policies in the last five years.

The average daily pattern shown by the different OA sources in winter (Figure 9) resembles that of BC, nitrate, sulphate and ammonium (Figure 5), with an increase of pollutants concentrations starting at around 10h UTC and reaching high concentrations at around 13h UTC. This daily increase is attributed to the transport from populated areas to the mountain site with the breeze. This variation is observed for all the components and therefore the local formation of SOA is deduced to be low in winter."

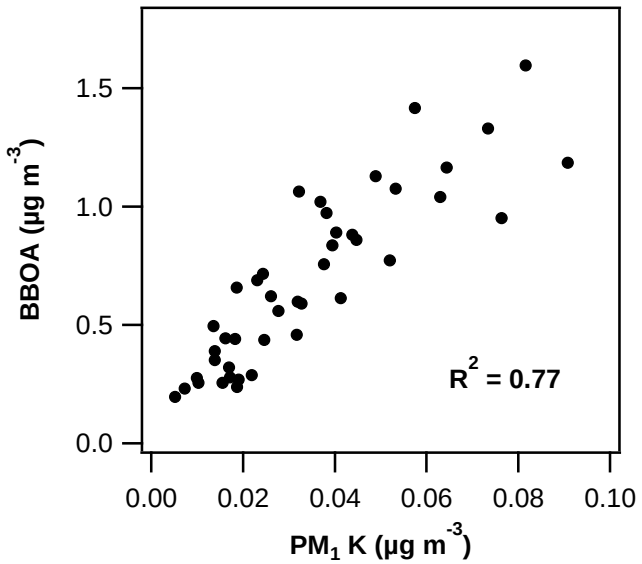

Figure S11. Contribution of BBOA in winter (averaged to 24-h periods matching the filter sampling) vs potassium concentrations in PM_1.

Reviewer#1. Technical correction 1) P967, L6: Carbonaceous aerosols are comprised of…

Reply to Reviewer#1. Technical correction 1)

It has been corrected.

Reviewer#1. Technical correction 2) P968, L21: …was estimated to be (instead of "estimated in")

Reply to Reviewer#1. Technical correction 2)

It has been corrected.

Reviewer#1. Technical correction 3) P970, L2: …the Azores, highly favors… (instead of "high")

Reply to Reviewer#1. Technical correction 3)

The authors meant that the entry of clean Atlantic air masses is favoured by the Azores high. To avoid confusion, the text has been edited as follows: "…the location of the Azores high pressure system favours the entry of clean Atlantic air masses…"

Reviewer#1. Technical correction 4) P975, L5: It is not clear whether the comparisons are made before or after the ACSM components concentrations are calculated using the time-dependent collection efficiency or from the raw data. Because, how can it be that slope between the sum of the ACSM+BC is very close to unity compared to the PM1 concentrations from the OPC (which is corrected with the 24h gravimetric measurements) but ammonium from the ACSM is almost double, nitrate is 2.8 times higher and organic matter is 4.25 times higher than the OC from the filters?

Reply to Reviewer#1. Technical correction 4)

The comparison of the concentrations of the ACSM components with the concentrations measured on filters was made after applying the time-dependent collection efficiency. The apparent discrepancy between the slopes obtained for ACSM+BC vs PM_1 from OPC (corrected with gravimetric measurements) and the slopes for the different components is attributed to the undetermined fraction of PM_1 mass in the filters. Thus, whereas the ACSM+BC concentrations are strictly the sum of the components, the PM_1 concentrations include a fraction of undetermined mass, partially attributed to water. The following clarification has been added to the main text in the revised manuscript together with a figure illustrating this explanation in the supplementary material:

"The apparent discrepancy between the slope for total PM_1 (ACSM+BC vs PM_1 from OPC corrected with gravimetric measurements, close to unity) and the slopes for the different components (>1) is attributed to the undetermined fraction of PM_1 mass in the filters. Thus, whereas the ACSM+BC concentrations are strictly the sum of the components, the PM_1 gravimetric concentrations include a fraction of undetermined mass, partially attributed to water (Figure S5)."

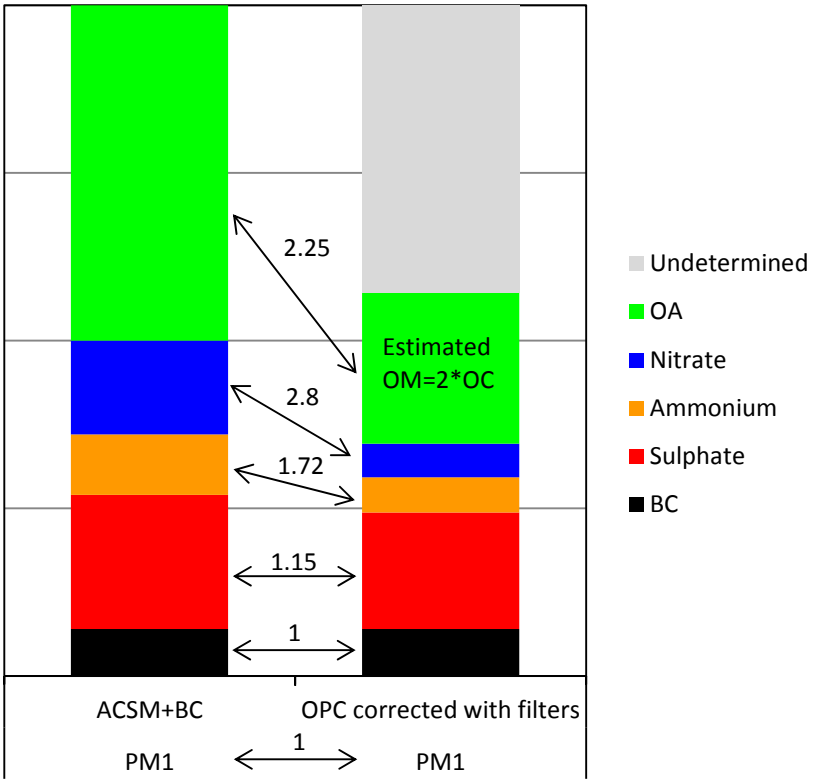

Figure S5. Schematic comparison of ACSM components + BC concentrations vs PM_1 concentrations from OPC corrected with gravimetric determinations. The numbers indicate the slopes found for experimental data for Montseny during June 2012 to July 2013. The 2.25 corresponds to the slope of OA (ACSM) vs OM estimated from OC (filters) as 2*OC.

<u>Reviewer#1. Technical correction 5)</u> P975, L12: It is stated that the slopes of sulphate and ammonium are relatively close to unity. For suplhate this may be the case (1.15) but for ammonium, I wouldn't call 1.72 close to unity, as it is closer to be the double.

<u>Reply to Reviewer#1. Technical correction 5)</u>

The text related to the discussion of the slopes has been changed as follows:

"For the strongly-correlated species, the slopes (ACSM vs off-line measurements) were different for each of them. Whereas it was close to unity for sulphate (1.15), it was higher for ammonium (1.72), and much higher for nitrate (2.80). The final reasons for this discrepancy remain unexplained, although a possible cause is the volatilization of ammonium nitrate from the filters."

<u>Reviewer#1. Technical correction 6)</u> P975, L20-25: Based on Aiken et al. (Environ. Sci. Technol. 42, 4478-4485, 2008) an estimate is proposed in order to calculate the OM-to-OC ratio base on the f44. Was this estimate used in order to see whether it compares to the slope obtained? Even though indeed, SOA is expected to have a high contribution at Montseny, I wouldn't expect a conversion factor for OC to OM higher than 2.2-2.4.

Reply to Reviewer#1. Technical correction 6)

The calculation of OM-to-OC ratio from the f44 based on Aiken et al. (2008) is not suitable for ACSM instruments, as recently learnt from an intercomparison of 13 Q-ACSM instruments (Fröhlich et al., 2015, Atmos. Meas. Tech. Discuss. 8, 1559-1613). During this intercomparison exercise, different f44 values were recorded by the different ACSM instruments, although they all followed the same trend. Therefore, the study concluded that in absence of specific calibration with organic standards, the calculation of O:C values (and OM:OC) from the f44 should be done with caution. Consequently the authors decided not to calculate the OM-to-OC ratios from the f44 in the present study. It should be noted that the intercomparison study also concluded that the precision of an individual, stable instrument is good and relative changes observed can be unambiguously interpreted, and that the source apportionment analyses are not compromised, and the influence on the mass contributions of the organic sources calculated with ME2 are minor. To include such clarifications, the following text has been added in the end of section 3.1 in the revised manuscript:

"The calculation of OM-to-OC ratio from the f44 based on Aiken et al. (2008) was not carried out given that it is not suitable for ACSM instruments, as recently learnt from an intercomparison of 13 Q-ACSM instruments (Fröhlich et al., 2015)"

It is true that the 4.25 ratio is very high, even for pure SOA, and it is higher than the OM-to-OC ratio determined for Montseny in March 2009 (Minguillón et al., 2011, Atmos. Chem. Phys. 11, 12067-12084). That is why two possible hyphotesis about why we obtain this high ratio are discussed in the manuscript. The discussion in the revised manuscript has been modified to include the OM-to-OC ratio determined for Montseny in March 2009:

"This large OM-to-OC ratio suggests photochemically well-aged organics, but it is too high even for a pure SOA (Aiken et al., 2008), which is expected to have an important contribution at MSY as will be discussed later (section 3.5), and it is higher than the OM-to-OC ratio determined in March 2009 at Montseny (2.0) (Minguillón et al., 2011). This extremely large OM-to-OC ratio might be attributed to…"

Reviewer#1. Technical correction 7) P977, L20: …due to shipping emissions (delete "the")

Reply to Reviewer#1. Technical correction 7)

It has been corrected.

Reviewer#1. Technical correction 8) P981, L15-16: Apart from the MAAP, is there an aethalometer available at Montseny station, in order to get and estimate on BC source apportionment? I would expect correlations with BC from fossil fuel and/or BC from wood burning to be higher.

Reply to Reviewer#1. Technical correction 8)

There are in fact aethalometer data available for this period at Montseny, but the dataset has not been assessed and interpreted thoroughly yet, as it will be the focus of future publications. Nevertheless, a preliminary data treatment is available and the BCff (BC from fossil fuel) and BCwb (BC from wood burning) have been estimated (Marco Pandolfi, from IDAEA-CSIC, is acknowledged for this). The results are encouraging, in the sense that the BCwb time series shows a meaningful seasonality, with higher values during the colder period. However, the BC due to biomass burning contributions at Montseny is very low on average, and hence the aethalometer method to separate this BCff and BCwb may not work as accurately as for areas with high biomass burning influence, such as the Alpine areas, from where the dataset was used to develop the method (Sandradewi et al., 2008, Environ. Sci. Technol. 42, 3316-3323). The authors did test the correlations of the preliminary estimated BCff with HOA, but the resulting correlation coefficients were similar or even worse than those for total BC. For example, for the warmer period, to which the reviewer makes reference to in the present comment, the HOA vs BC squared Pearson coefficient was 0.51, and the HOA vs BCff squared Pearson coefficient was 0.44. Consequently, given the fact that the aethalometer results are still preliminary, the authors decided not to include such information in the present paper.

Reviewer#1. Technical correction 9) Figure S6: What is the difference between the two diagrams in the bottom? Because all axes and annotations are the same. From what I gather, the panel in the left seems to be the so-called Aged BBOA and not the BBOA.

Reply to Reviewer#1. Technical correction 9)

The figure in the right meant to be a zoom from figure in the left, with the scale from 0.00 to 0.03, in order to show better the *m/z* with low contributions to the factor, mainly the *m/z* 60, with high relevance for the biomass burning profile. It has been now explained in the figure caption as follows:

"Figure S9. Comparison of the BBOA factor found for the wildfire episode (BBOA_MSY) with other BBOA profiles found in the literature (Minguillón et al., 2011;Ng et al., 2011;Crippa et al., 2013). The scatter plot on the right is a zoon for values from 0.00 to 0.03."

Reviewer#2. In this manuscript, the authors report on 2-month field campaign deploying an ACSM and MAAP and describe their measurements against mass, organic carbon, and elemental composition obtained with collocated PM1 filter measurements. After describing the choices for constrained and unconstrained parameters, the results of the ACSM with respect to organic aerosol fraction, speciation, and sources for the region are discussed. The authors synthesize a large quantity of information and present new and interesting evaluations for the ACSM. The basis of the work is of sound quality and the topic is relevant for readers of Atmospheric Chemistry and Physics, and is therefore recommended for publication. There are several points which are recommended for consideration before publication.

Reviewer#2. General comment 1) Can the RIE and CE be assessed independently of one another? In the case of external mixing, the acidity-corrected CE may not apply to that of organics (as reported by Hawkins and Russell, 2010), and quartz fiber filters are known to have adsorption artifacts (though this would not help the argument of extremely high OA/OC ratio).

Hawkins, L. N., L. M. Russell, D. S. Covert, P. K. Quinn, and T. S. Bates. "Carboxylic Acids, Sulfates, and Organosulfates in Processed Continental Organic Aerosol over the Southeast Pacific Ocean during VOCALS-REx 2008." Journal of Geophysical Research 115, no. D13 (July 2, 2010). doi:10.1029/2009JD013276.

Reply to Reviewer#2. General comment 1)

The CE was applied to the total mass spectra and therefore it affected equally all the components of the atmospheric aerosol. This was done according to the agreement within the European ACTRIS-ACSM community (http://www.actris.net) to apply the CE to the whole mass spectra preferably using the Middlebrook approach (http://www.psi.ch/acsm-stations/acsm-best-practice). Nevertheless, the authors are aware that the Middlebrook approach only works if the particles are internally mixed. At Montseny, a regional background site, it is reasonable to assume that the particles are internally mixed, and hence the application of a unique CE would be suitable. This assumption has been explained in section 2.2 (ACSM settings, calibrations and data processing) in the revised manuscript as follows:

"The aerosols at MSY are assumed to be internally mixed and thus the CE was assumed to be the same for different components in contrast to e.g. Hawkins et al. (2010)."

Reviewer#2. General comment 2) Is the ACSM PM1 + BC expected to match the PM1 so well (slope ~1)? I.e., was there indication of the level of mineral dust in the PM1 samples with the ICP-MS?

Reply to Reviewer#2. General comment 2)

From the ICP analyses carried out with the PM_1 filter samples, the mineral matter in PM_1 was below 0.3 μg m^{-3} for all the sampling period except for eleven specific days with a strong influence of Saharan dust, which affected also the PM_1 fraction. For six of these days, the mineral matter concentration ranged from 0.3 μg m^{-3} to 1 μg m^{-3}, and only for the remaining five days the mineral matter concentration ranged from 1 μg m^{-3} to 2 μg m^{-3}. Likewise, the sea spray contribution was below the detection limit of 0.25 μg m^{-3}. Therefore, there are no major contributors to PM_1 mass other than the ACSM components and the BC for the sampling period at Montseny.

Reviewer#2. General comment 3) An approximate OM/OC ratio for ACSM alone can be calculated independently of the filter OC based on the parameterization of Aiken et al. (2008) assuming the same instrument response; it may be worth discussing ACSM OC vs. filter OC or ACSM OA vs. filter OA to focus the problem on the sampling artifacts.

Reply to Reviewer#2. General comment 3)

The calculation of OM-to-OC ratio from the f44 based on Aiken et al. (2008) is not suitable for ACSM instruments, as recently learnt from an intercomparison of 13 Q-ACSM instruments (Fröhlich et al., 2015, Atmos. Meas. Tech. Discuss. 8, 1559-1613). During this intercomparison exercise, different f44 values were recorded by the different ACSM instruments, although they all followed the same trend. Therefore, the study concluded that in absence of specific calibration with organic standards, the calculation of O:C values (and OM:OC) from the f44 should be done with caution. Consequently the authors decided not to calculate the OM-to-OC ratios from the f44 in the present study. It should be noted that the intercomparison study also concluded that the precision of an individual, stable instrument is good and relative changes observed can be unambiguously interpreted, and that the source apportionment analyses are not compromised, and the influence on the mass contributions of the organic sources calculated with ME2 are minor. To include such clarifications, the following text has been added in the end of section 3.1 in the revised manuscript:

"The calculation of OM-to-OC ratio from the f44 based on Aiken et al. (2008) was not carried out given that it is not suitable for ACSM instruments, as recently learnt from an intercomparison of 13 Q-ACSM instruments (Fröhlich et al., 2015)"

Reviewer#2. General comment 4) As pointed out in Canonaco et al. (2013) and others, the apportionment of HOA, OOA, BBOA, etc. may be sensitive to the constraints imposed by the matrix decomposition. As pointed out by reviewer #1, it would be relevant to discuss the ME-2 solutions and potential uncertainties in the reported values, or discuss ranges which have been reported in the literature such that it is clear which conclusions are robust and which are subject to the assumptions of the decomposition.

Reply to Reviewer#2. General comment 4)

The discussion on the chosen PMF solution has been extended. Please refer to the Reply to Reviewer#1. Specific comment 4) for an explanation and the text included in the revised manuscript.

Reviewer#2. Minor comment 1) The authors do not mention the f60 ratios of the BBOA factors of the wildfire period.

Reply to Reviewer#2. Minor comment 1)

The discussion on the wildfire event has been changed and it directly states now the f60 values of the different BBOA profiles. The part of the text making reference to f60 reads as follows:

"The BBOA_MSY profile found here is very similar to a BBOA profile found for Montseny in March 2009 (Minguillón et al., 2011) (https://sites.google.com/site/amsglobaldatabase) and to an average profile for BBOA from various datasets (Ng et al., 2011a) (Figure S9). The f60 in the BBOA_MSY factor is 0.014, similar to the f60 in these other two BBOA profiles (0.017 and 0.024). It has been also compared to the BBOA found in the background of Paris (Crippa et al., 2013), with which some more differences were found, mainly our profile has higher *m/z* 43 and *m/z* 41 signals and lower *m/z* 60 (Figure S9)."

Reviewer#2. Minor comment 2) Figure 2. The authors may wish to write the equation y = a + bx in the caption such that parameters "a" and "b" in the panels can be interpreted as intercept and slope.

Reply to Reviewer#2. Minor comment 2)

The equation has been included in the figure caption.

Chemical characterization of submicron regional background aerosols in the Western Mediterranean using an Aerosol Chemical Speciation Monitor

M.C. Minguillón[1], A. Ripoll[1,2], N. Pérez[1], A.S.H. Prévôt[3], F. Canonaco[3], X. Querol[1], A. Alastuey[1]

[1]Institute of Environmental Assessment and Water Research (IDAEA-CSIC), Jordi Girona 18-26, Barcelona, 08034, Spain

[2]Departament d'Astronomia i Meteorologia, Universitat de Barcelona, Martí i Franquès 1, 08028, Barcelona, Spain

[3]Paul Scherrer Institute, Laboratory of Atmospheric Chemistry, 5232 Villigen PSI, Switzerland

*Corresponding author: mariacruz.minguillon@idaea.csic.es

ABSTRACT

An Aerosol Chemical Speciation Monitor (ACSM, Aerodyne Research Inc.) was deployed at Montseny (MSY, 720 m a.s.l.) regional background site in the Western Mediterranean from June 2012 to July 2013 to measure real-time inorganic (nitrate, sulphate, ammonium and chloride) and organic submicron aerosol concentrations. Co-located measurements were also carried out including real-time submicron particulate matter (PM_1) and black carbon (BC) concentrations, and off-line PM_1 chemical analysis. This is one of the few studies that compare ACSM data with off-line PM_1 measurements, avoiding the tail of the coarse mode included in the $PM_{2.5}$ fraction. The ACSM + BC concentrations agreed with the PM_1 measurements, and strong correlation was found between the concentrations of ACSM species and the off-line measurements, although some discrepancies remain unexplained. Results point to a current underestimation of the relative ionization efficiency (RIE) established for organic aerosol (OA), which should be revised in the future. The OA was the major component of submicron aerosol (53% of PM_1), with a higher contribution in summer (58% of PM_1) than in winter (45% of PM_1). Source apportionment of OA was carried out by applying Positive Matrix Factorization (PMF) using the Multilinear Engine (ME-2) to the organic mass spectral data matrix. Three sources were identified in summer: hydrocarbon-like OA (HOA), low-volatile oxygenated OA (LV-OOA), and semi-volatile oxygenated OA (SV-OOA). The secondary OA (SOA, 4.7 μg m^{-3}, sum of LV-OOA and SV-OOA) accounted for 85% of the total OA and its formation during daytime (mainly SV-OOA) was estimated to be 1.1 μg m^{-3}. In winter, HOA was also identified (12% of OA), a contribution from biomass burning OA was included, and it was not possible to differentiate two different SOA factors but a single OOA factor was resolved. The OOA contribution represented the 60% of the total OA, with a degree of oxidation higher than both OOA summer factors. An intense wildfire episode was studied obtaining a region-specific BBOA profile.

KEYWORDS: ACSM, PM_1, organics, chemical composition, Mediterranean, air quality.

1 INTRODUCTION

Ambient aerosols have adverse effects on human health (Pope III and Dockery, 2006), and affect climate (IPCC, 2013), ecosystems, crops, and regional visibility. Fine particulate matter (PM_1, particles with an aerodynamic diameter <1 μm) contains substantial fractions of inorganic compounds and carbonaceous aerosols, the latter reaching up to 90% of the mass (Jimenez et al., 2009). Carbonaceous aerosols are comprised of organic compounds, collectively referred to as organic aerosol (OA), elemental carbon (EC), and carbonates (from mineral dust), although the latter can be considered negligible in submicron aerosols.

The Western Mediterranean Basin (WMB) has special atmospheric and geographic characteristics that imply the interest of the detailed study of the ambient aerosols in this area (Querol et al., 2009). The regional background has been investigated through long data series of measurements in previous studies available at Montseny (representative of the regional background in the WMB). Pérez et al. (2008) found average particulate matter concentrations at Montseny of 17, 13 and 11 μg m^{-3} of PM_{10}, $PM_{2.5}$ and PM_1, respectively, in the 2002-2007 period. Cusack et al. (2012) and Querol et al. (2014) found a decreasing trend in $PM_{2.5}$ concentrations from 2001 to 2012 of −0.39 μg m^{-3} per year. $PM_{2.5}$ concentrations were found higher in the WMB than at other rural background sites across Spain, Portugal, Germany and Scandinavia but lower than those measured in Switzerland, Italy and Austria (Cusack et al., 2012). The prevailing daily evolution is driven by the breeze circulation (mountain and sea breezes), with lower PM_x concentrations at night owing to the nocturnal drainage flows, and higher PM_x concentrations at midday owing to the transport of atmospheric pollutants accumulated in the pre-coastal depression upwards by the breeze (Pérez et al., 2008). Maximum PM_{10} concentrations were found in summer, February-March and November, and sporadic PM_x increases may be recorded under anticyclonic conditions (Pey et al., 2010). The chemical composition of $PM_{2.5}$ is characterised by high concentrations of organic aerosol and sulphate, followed by crustal material, nitrate and ammonia, with sea spray and elemental carbon being a minor part of the total $PM_{2.5}$ mass (Cusack et al., 2012). Compared to other central European sites, the Western Mediterranean aerosol is characterised by higher concentrations of crustal material but lower concentrations of organic aerosol, elemental carbon and ammonium nitrate (Pey et al., 2009). Nevertheless, relatively high $PM_{2.5}$ concentrations of carbonaceous aerosol and sulphate transported from populated coastal areas are regularly recorded, especially during winter anticyclonic episodes and summer midday PM highs (Pey et al., 2009;Pey et al., 2010). A organic carbon (OC) to elemental carbon (EC) ratio (14 in summer, 10 in winter) was detected, pointing to the influence of biogenic

Código de campo cambiado

emissions, secondary organic aerosol (SOA) formation favoured by high ozone concentrations and insolation, and intensive recirculation of aged air masses (Pey et al., 2009;Querol et al., 2013).

The sources of organic aerosol in the regional background site of Montseny were studied in two intensive campaigns, using off-line ^{14}C analysis (Minguillón et al., 2011), Aerosol Mass Spectrometers (AMS) (Minguillón et al., 2011;Crippa et al., 2014), and organic tracers (Alves et al., 2012;Van Drooge et al., 2012). Minguillón et al. (2011) found that the contribution of fossil fuel combustion sources (mainly road traffic emissions) to OC at Montseny was 31% and 25%, in winter and summer, respectively, and that 85% of this fossil OC was secondary. The contribution of biomass burning emissions was relatively low when compared with other regional background sites in Europe, and was estimated to be 21% and 12% of the total OC in winter and summer, respectively. Alves et al. (2012) concluded that the anthropogenic input may be associated with the transport of aged air masses from the surrounding industrial/urban areas, which superimpose the locally originated biogenic hydrocarbons.

Besides these studies, a long time series of organic aerosol data has not been analysed in Montseny. To this end, the newly-developed Aerosol Chemical Speciation Monitor (ACSM) would be suitable (Ng et al., 2011b), as opposed to the use of AMS, which cannot work unattended and therefore is usually employed around the world for periods of about one month. Nevertheless, due to its recent implementation, some studies based on ACSM data are found in the literature (Ng et al., 2011b;Shaw et al., 2012;Sun et al., 2012;Budisulistiorini et al., 2013;Canonaco et al., 2013;Carbone et al., 2013;Sun et al., 2013a;Sun et al., 2013b;Takahama et al., 2013;Bougiatioti et al., 2014;Canonaco et al., 2014;Petit et al., 2014;Ripoll et al., 2014a).

The present study aims at interpreting a one-year time series of inorganic and organic compounds in the submicron aerosol in the regional WMB, with special focus on their evolution throughout the year as a function of the concatenation of different atmospheric scenarios. The different types and origin of organic aerosol (OA) are also investigated. To this end, an ACSM was deployed for a year in the regional background site of Montseny (MSY), according to the schedule planned within the Aerosols, Clouds, and Trace gases Research InfraStructure (ACTRIS) Network project. Moreover, a validation of the ACSM data is carried out by comparison with co-located instruments both real-time and off-line.

Código de campo cambiado
Código de campo cambiado
Código de campo cambiado
Código de campo cambiado
Código de campo cambiado
Código de campo cambiado
Código de campo cambiado
Código de campo cambiado
Eliminado: in
Código de campo cambiado
Código de campo cambiado
Código de campo cambiado
Código de campo cambiado
Código de campo cambiado
Código de campo cambiado
Código de campo cambiado
Código de campo cambiado
Código de campo cambiado
Código de campo cambiado
Código de campo cambiado
Código de campo cambiado
Código de campo cambiado
Código de campo cambiado

2 METHODOLOGY

2.1 Sampling site

The MSY station (41°46'46"N, 02°21'29"E, 720 m a.s.l.) is located in the Montseny natural park, in a densely forested area, 50 km to the N-NE of the Barcelona urban area, and 25 km from the Mediterranean coast. The station is located on the upper walls of a valley extending perpendicularly from the Catalan Pre-Coastal ranges to the coast. The site is relatively far from urban and industrial areas, but it can be affected by anthropogenic emissions transported from populated and industrialised areas under specific meteorological conditions. The MSY station is in the ACTRIS Network (formerly EUSAAR, European Supersites for Atmospheric Aerosol Research), is a Global Atmosphere Watch (GAW) site, and is part of the IDAEA-CSIC and the Department of Environment of the Autonomous Government of Catalonia air quality monitoring network.

The prevailing atmospheric dynamics has been described elsewhere (Pérez et al., 2008;Pey et al., 2009). Briefly, in winter the location of the Azores high pressure system favours the entry of clean Atlantic air masses into the WMB which replace the existing air masses leading to a decrease of pollutants. In summer, the very weak pressure gradients result in local circulations dominating the atmospheric dynamics with the consequent accumulation of pollutants (Millán et al., 1997). The climate is typical Mediterranean with warm summers, temperate winters and irregular precipitation rates during the year.

The daily classification of meteorological episodes affecting MSY during the study period was made as described in Pérez et al. (2008), leading to the following types of scenario: Atlantic Advection, North African, Mediterranean, European, Regional, and Winter Anticyclonic Episodes. The frequency of each type of scenario for each of the months of the study period is shown in Figure S1.

2.2 ACSM settings, calibrations and data processing

An ACSM was deployed from June 2012 to July 2013, according to the ACTRIS schedule, to measure non-refractory submicron aerosol species (organics, nitrate, sulphate, ammonium and chloride) in real-time (Ng et al., 2011b). Briefly, the instrument uses an aerodynamic lens to sample and focus submicron particles (75-650 nm) into a narrow particle beam (Liu et al., 2007), with a flow of approximately 85 cc/min. The beam is transmitted into the final of three vacuum chambers, where particulate matter is flash-vaporized on a hot oven (600 °C), ionized by hard electron impact ionization (70eV) and subsequently detected using a

Código de campo cambiado

Código de campo cambiado

Código de campo cambiado

Código de campo cambiado

Eliminado: Figure S1

Código de campo cambiado

Código de campo cambiado

commercial quadrupole mass spectrometer. The concentration of the aforementioned species is calculated based on the measured aerosol mass spectra. For a given species, its concentration is calculated based on the addition of the ion signals at each of its mass spectral fragments and its ionization efficiency (IE) (Canagaratna et al., 2007). Since calibration of IEs for all ambient species is not feasible, the relative ionization efficiency (RIE) (compared to that of nitrate) is used for different species.

Thus, mass calibration of the ACSM is based on determining the instrument response factor (RF) using ammonium nitrate calibration aerosol (Ng et al., 2011b). In this study, an atomizer (TSI, Constant Output Atomizer Model 3076) was used for primary aerosol generation, followed by a silica gel diffusion dryer, an SMPS system (model TSI 3936), comprised of an electrostatic classifier (model TSI 3080) with a differential mobility analyzer (DMA, model TSI 3081) and a condensation particle counter (CPC, TSI 3772). Monodisperse 300 nm ammonium nitrate aerosol particles were generated for the calibration. The calibration comprised a range of nitrate concentrations from 0 to 15 μg m^{-3}, which were achieved by diluting the generated aerosol. RIE for ammonium was directly determined from the ammonium nitrate calibration.

Several calibrations were carried out through the sampling period, and average values for nitrate IE and RIE for ammonium were used for the whole dataset. After several tests around the world, more experience has been gained regarding the performance of the ACSM. Hence, RIE for sulphate has been shown to vary from instrument to instrument and therefore the default value (1.2) (Ng et al., 2011b) cannot be directly used. Nevertheless, this information was known when our ACSM was no longer at the MSY station, and hence, sulphate RIE was determined by doing the aforementioned calibration exercise with ammonium sulphate monodisperse aerosol in Barcelona. The sulphate RIE value found was very close to the default value and hence 1.2 was used for the current dataset. The default RIE for organics (1.4) (Ng et al., 2011b) has been used, although some discussion about this can be found in section 3.1.

The ACSM was connected to a general inlet equipped with a nafion drier to maintain the RH below 40%, although technical problems resulted in some periods (about 50% of the data points) with uncontrolled RH. The ACSM was set to measure with a time resolution of approximately 30 minutes, resulting from setting it to work with 24 scans (alternatively 1 sample and 1 filtered) per data point with a scan speed of 500 ms/amu. The data acquisition software provided by Aerodyne Research (version 1.4.2.5 from the beginning to 18th December 2012, and version 1.4.3.8 for the rest of the period) was used to process the measurements. The data were analyzed with the ACSM data analysis software version 1.5.3.2 (Aerodyne

Código de campo cambiado

Código de campo cambiado

Código de campo cambiado

Código de campo cambiado

Research Inc.) written in Igor Pro (WaveMetrics, Inc., Lake Oswego, OR, USA). A correction for the instrument performance limitations was applied to the dataset based on the inlet pressure and N_2 signal. The aerosol mass concentrations were then corrected for particle collection efficiency (CE) following the Middlebrook approach (Middlebrook et al., 2012). The aerosols at MSY are assumed to be internally mixed and thus the CE was assumed to be the same for different components in contrast to e.g. Hawkins et al. (2010).

2.3 Additional measurements and instrumentation

Submicron particulate matter (PM_1) 24-h samples were collected on quartz fibre filters (Pallflex 2500QAT-UP) using DIGITEL (DH-80) high volume (30 m^3 h^{-1}) samplers with a PM_1 impactor inlet. The sampler, and therefore the collected samples, was kept inside a container with controlled temperature (between 24 and 26°C). Samples were collected every 4 days. Gravimetric PM_1 determination was carried out by weighing the filters before and after sampling, after stabilization in a conditioned room (20°C and 50% relative humidity). Chemical off-line analyses were carried out. A quarter of the filter was acid digested (HNO_3:HF:$HClO_4$), and the resulting solution was analysed by Inductively Coupled Plasma Atomic Emission Spectroscopy (ICP-AES) for major elements determination, including S, from which the sulphate concentration was calculated. Another quarter of the filter was water extracted to determine the nitrate, sulphate and chloride concentrations by Ion Chromatography and the ammonium concentrations by an ion selective electrode. OC concentrations were determined by thermal-optical methods using a Sunset instrument following the EUSAAR2 thermal protocol (Cavalli et al., 2010). Blank filters were analysed together with the samples and concentrations were subtracted from those found in the samples in order to calculate the ambient concentrations.

PM_1 hourly concentrations were measured using an optical particle counter (GRIMM, model 180) and corrected with the simultaneous 24-h gravimetric measurements (Alastuey et al., 2011). Equivalent Black Carbon (BC) mass concentrations (Petzold et al., 2013) were measured with a 1-minute time resolution by a multi-angle absorption photometer (MAAP, model 5012, Thermo) using a PM_{10} inlet, and using the default mass absorption cross section (MAC) from the instrument software (6.6 m^2 g^{-1}). Particle number size distributions (9-820 nm) were measured by a Scanning Mobility Particle Sizer (SMPS), comprising a DMA connected to a CPC (TSI 3772), with a system designed and manufactured at the Leibniz Institute for Tropospheric Research (Wiedensohler et al., 2012). The mass concentration from SMPS data

Código de campo cambiado
Eliminado: and
Eliminado: c
Código de campo cambiado
Código de campo cambiado
Código de campo cambiado
Código de campo cambiado

was calculated from the total volume of particles and the composition-dependent density calculated basedon the ACSM chemical composition.

Wind direction and speed, solar radiation, temperature, relative humidity and precipitation were recorded using conventional instruments and hourly data can be seen in Figure S2.

Eliminado: Figure S2

2.4 Source apportionment of OA

The source apportionment to the organic fraction can be investigated by applying Positive Matrix Factorization (PMF) (Paatero and Tapper, 1994) using the Multilinear Engine (ME-2) (Paatero, 1999) to the organic mass spectra. Both methods describe the measurements with a bilinear factor model:

Código de campo cambiado

Código de campo cambiado

$$x_{ij} = \sum_{k=1}^{p} g_{ik} f_{kj} + e_{ij} \quad (1)$$

where x_{ij} is the j^{th} species (m/z) concentration measured in the i^{th} sample, p is the number of sources, g_{ik} is the contribution of the k^{th} source to the i^{th} sample, f_{kj} is the concentration of the j^{th} species in the k^{th} source (mass spectra) and e_{ij} is the residual associated with the j^{th} species concentration measured in the i^{th} sample. The values g_{ik} and f_{kj} are adjusted until a minimum for the objective function Q for a given number of factors p is found:

$$Q = \sum_{i=1}^{n} \sum_{j=1}^{m} \left(\frac{e_{ij}}{\sigma_{ij}} \right)^2 \quad (2)$$

where σ_{ij} is the user defined uncertainty for the j^{th} species in the i^{th} sample.

With the ME-2, the user can introduce a priori information about sources e.g. using the so-called a-value approach. Hence, the user inputs one or more factor profiles and a constraint defined by the a-value, which determines the extent to which the output profile can differ from the profile fed to the model.

In the present study the source apportionment to OA was performed applying ME-2 using the toolkit SoFi (Source Finder) version 4.7 described in Canonaco et al. (2013). The ME-2 was applied separately for the warm and cold periods in this study, given the expected differences among them. The warm period was defined as a period with >70% of the days with average T>19°C, hourly max T>24°C and hourly min T>15°C, which includes 14th June to 9th October 2012. The cold period was defined as a period with >70% of the days with average T<10°C, hourly max T<13°C and hourly min T<8°C and includes 28th October 2012 to 7th April 2013. Only m/z<=100 were used for several reasons: a) the signals of m/z>100 account for a

Código de campo cambiado

minor fraction of the total signal (2% on average), b) the *m/z*>100 have larger uncertainties, and c) the large interference of naphthalene signals (at *m/z* 127, 128, and 129) is avoided. The error matrix was calculated by the aforementioned customized software, which downweights the *m/z* masses calculated from the *m/z* 44 signal. Moreover, *m/z* with signal to noise ratio (S/N) below 0.2 were downweighted by a factor of 10, and those with S/N between 0.2 and 1 were downweighted by a factor of 2.

3 RESULTS AND DISCUSSION

3.1 Comparison of ACSM data with other measurements

This is one of the few studies, together with Ripoll et al. (2014a), that compare ACSM data with off-line PM_1 measurements. Most of the studies found in the literature comparing ACSM data with off-line measurements are based in the $PM_{2.5}$ fraction for the off-line measurements. In this study we use PM_1 measurements, avoiding the tail of the coarse mode that the $PM_{2.5}$ fraction includes, and hence being closer to the size range measured by the ACSM (75-650nm).

The sum of the ACSM components concentrations and the BC concentrations measured by the MAAP was compared with PM_1 concentrations determined by the optical particle counter, resulting in a strong correlation (squared Pearson correlation coefficient, R^2=0.66) and a slope very close to unity (1.005) (Figure 1). The application of a time-dependent collection efficiency (CE) to the ACSM data based on the Middelbrook approach (Middlebrook et al., 2012) resulted in a better fit compared to the use of a constant CE=0.5 used in several studies (which resulted in a slope of 0.913 and a R^2=0.65). Hence the time-dependent CE application is considered more suitable for the present study. The time-dependent CE equalled the default value of 0.45 for most of the period, and increased up to 0.65 during the colder period (Figure S3). The sum of ACSM components and BC concentrations was also compared to the mass concentration calculated from SMPS data, resulting in a strong correlation (squared Pearson correlation coefficient, R^2=0.77) and a slope very close to unity (0.997) (Figure S4). Moreover, ACSM components concentrations were daily averaged and compared to off-line measurements from 24-h PM_1 samples (Figure 2). All the species, except for chloride, showed strong correlations (R^2 of 0.68, 0.82 and 0.94 for ammonium, nitrate and sulphate, respectively). Chloride concentrations were below or close to detection limits for both ACSM and off-line analysis, which may be the cause for the discrepancies found. Such discrepancies were also found in other studies (Budisulistiorini et al., 2014). For the strongly-correlated

Código de campo cambiado

Eliminado: Figure 1

Código de campo cambiado

Con formato: Superíndice

Eliminado: Figure 2

Código de campo cambiado

species, the slopes (ACSM vs off-line measurements) were different for each of them. Whereas it was close to unity for sulphate (1.15), it was higher for ammonium (1.72), and much higher for nitrate (2.80). The final reasons for this discrepancy remain unexplained, although a possible cause is the volatilization of ammonium nitrate from the filters. Nevertheless, the volatilization of ammonium nitrate is expected to be low given that the samples are kept at controlled conditions (24-26°C) as described in the methods section. Moreover, if random volatilization occurred, the correlation coefficients found between ACSM and filters would be lower. The apparent discrepancy between the slope for total PM_1 (ACSM+BC vs PM_1 from OPC corrected with gravimetric measurements, close to unity) and the slopes for the different components (>1) is attributed to the undetermined fraction of PM_1 mass in the filters. Thus, whereas the ACSM+BC concentrations are strictly the sum of the components, the PM_1 gravimetric concentrations include a fraction of undetermined mass, partially attributed to water (Figure S5).

For organic aerosol a strong correlation was found (R^2=0.82), and the high slope obtained (4.25) may be interpreted as the OM-to-OC ratio, since the ACSM measures OA and the off-line measurements determined OC. This large OM-to-OC ratio suggests photochemically well-aged organics, but it is too high even for a pure SOA (Aiken et al., 2008), which is expected to have an important contribution at MSY as will be discussed later (section 3.5), and it is higher than the OM-to-OC ratio determined in March 2009 at Montseny (2.0) (Minguillón et al., 2011). This extremely large OM-to-OC ratio might be attributed to a) underestimation of OC due to loss of semi-volatile organic compounds from the filters, and b) overestimation of OM by the ACSM due to an underestimation of the RIE for organics. The first reason is expected to be less likely given the strong correlation found between OA and OC (which would not be so if random volatilization occurred) and given that the samples are kept at controlled conditions, as formerly explained, hence reducing the possible volatilization. Previous studies also found higher than expected OM-to-OC ratios when comparing ACSM OA with off-line OC measurements. Budisulistiorini et al. (2014) found OM-to-OC ratios of 4.85 and 3.85 in summer and fall, respectively. Ripoll et al. (2014a) found an OM-to-OC ratio of 3.39 for a one year sampling period. This topic is currently being investigated by the ACSM manufacturer. The calculation of OM-to-OC ratio from the f44 based on Aiken et al. (2008) was not carried out given that it is not suitable for ACSM instruments, as recently learnt from an intercomparison of 13 Q-ACSM instruments (Fröhlich et al., 2015).

Eliminado: they were

Eliminado: relatively

Eliminado: and ammonium

Eliminado: and

Eliminado: , respectively

Eliminado: the slope was

Eliminado: (which is also reflected in the 1.72 slope obtained for ammonium)

Código de campo cambiado

Código de campo cambiado

Código de campo cambiado

Código de campo cambiado

Código de campo cambiado

3.2 Time series and average composition of submicron aerosol. Seasonal variation

The average concentration (P25, P75) of the ACSM components plus BC concentrations during the study period was 7.3 μg m^{-3} (3.1, 10.2). The highest concentrations were measured during the warm periods (average 10.3 μg m^{-3}), defined as the periods with most of the days with average T>20ºC (from 14th June to 9th October 2012 and from 13th June to 9th July 2013). The lowest concentrations were recorded during the cold period (average 5.8 μg m^{-3}), which includes a period with most of the days with average T<13ºC (from 28th October 2012 to 7th April 2013) (Figure 3). The average monthly concentrations, following the described variation, can be seen in Figure 4. This is in agreement with the seasonal variations observed during a long time period (2002-2010) by Cusack et al. (2012). The summer increase is associated with the recirculation of air masses that prevent air renovation, the low precipitation (Figure S2), and the formation of secondary aerosols enhanced by the maximum solar radiation (Figure S2). The lower winter concentrations can be explained by the high frequency of Atlantic advections (Figure S1) and the higher precipitation rates, although occasional high concentrations are attributed to winter anticyclonic scenarios (Pey et al., 2010). The seasonal variation of PM_1 concentrations at MSY is also influenced by the evolution of the boundary layer height, which is lower during wintertime and increases during summertime, especially during the central hours of the day. Changes in the origin of air masses also determined the seasonal variation of PM_1 concentrations.

On average, the most abundant component was OA (3.8 μg m^{-3}), followed, in this order, by sulphate (1.3 μg m^{-3}), ammonium (0.8 μg m^{-3}), nitrate (0.8 μg m^{-3}), BC (0.4 μg m^{-3}) and chloride (<0.1 μg m^{-3}). The OA contribution varied throughout the year, reaching 60% of the total PM_1 in the summer period (June, July and August) and decreasing progressively down to 43% in February (Figure 4). The contribution of sulphate followed the same seasonal variation, from about 20% in the warmer months to about 8% in the colder months. The nitrate contribution showed an inverse trend, with higher relative contributions in the winter and much lower in summer. These seasonal variations were already observed in previous studies using off-line filter sampling (Pey et al., 2009;Ripoll et al., 2014b) and can be attributed to a higher SOA contribution, favoured formation of sulphate, and nitrate gas/aerosol partitioning leading to vaporization of ammonium nitrate during the warmer period.

When investigating the diurnal patterns, it is observed that OA, nitrate and BC concentrations reach the maximum at around 14h UTC in summer, whereas sulphate and ammonium show a delayed increase in their concentrations, peaking at around 16h UTC (Figure 5). The reasons for this shift may obey to the different origin of each component.

Eliminado: Figure 3
Eliminado: Figure 4
Código de campo cambiado
Eliminado: Figure S2
Eliminado: Figure S2
Eliminado: Figure S1
Código de campo cambiado
Eliminado: Figure 4
Código de campo cambiado
Código de campo cambiado
Eliminado: Figure 5

Whereas the OA, nitrate and BC are transported with the breeze from the populated areas and the valley towards the regional background site, the sulphate can also be transported from further away, i.e. from over the Mediterranean Sea due to shipping emissions. Later in the day, when the breeze is developed in the opposite direction (from inland towards the coast), the concentrations of OA, BC and nitrate decrease, whereas the sulphate and ammonium concentrations remained high for longer time (until about 19h UTC). This is due to the more regional character of ammonium sulphate, which is present in a wider area due to its longer lifetime in the atmosphere (Seinfeld and Pandis, 2006) and hence remains longer at MSY. In addition to the transport of pollutants, local SOA can be formed (see section 3.5 for discussion). Specific episodes may differ from this average behaviour owing to specific atmospheric characteristics, for which sulphate concentrations increase simultaneously with OA, but the most common variation is the one described here. On the other hand, in winter, all the components show an increase at around 15h UTC, and concentrations remain high until around 22h UTC, when they start to decrease to reach a minimum around 9h UTC (Figure 5). This simultaneous variation indicates that the pollutants are transported from the nearby polluted areas to MSY with the breeze.

Eliminado: the

Código de campo cambiado

Eliminado: Figure 5

3.3 Influence of the type of scenario on submicron aerosol

The total PM_1 concentrations were investigated as a function of the type of scenario, finding the lowest concentrations during Mediterranean episodes and Atlantic advections, and the highest during North African outbreaks, European episodes and Winter Anticyclonic episodes (Figure 6). Some differences in the relative chemical composition as a function of the type of scenario were found (Figure 6). OA and sulphate relative contributions were higher under regional and North African episodes. This may be due to the higher formation of secondary aerosols enhanced by the higher temperature and solar radiation during these episodes. See additional discussion about formation of SOA in section 3.5. Moreover, the higher sulphate concentrations under regional episodes may also be due to the enhanced regional mixing, as shown by the flatter diurnal pattern shown for this pollutant (Figure S6). Sulphate relative contribution was also high when Mediterranean air masses affected MSY probably owing to the impact of shipping emissions. On the other hand, nitrate relative contribution was found to be higher for Winter Anticyclonic and European episodes. For both cases the colder weather compared to the rest of the year is partly responsible for the higher nitrate concentrations. During Winter Anticyclonic episodes, the stagnant conditions favouring the accumulation of polluted air masses that are transported from the Barcelona metropolitan

Eliminado: Figure 6

Eliminado: Figure 6

Eliminado: Figure S3

area towards MSY may also be responsible for the high nitrate concentrations (Pey et al., 2010). Note that this transport takes place later in the day than in warm conditions, thus reaching the maximum concentrations between 15h UTC and 22h UTC, and that the day-night difference is much higher than for other scenarios (Figure S6). During European episodes, the higher nitrate concentration can be attributed to the long range transport of nitrate from Europe to the study area, although this type of episodes often take place under anticyclonic conditions and hence the nitrate may have a local origin at lower heights, whereas European nitrate is transported at higher altitudes, as it was seen by Ripoll et al. (2014b).

The relative chemical composition as a function of the total concentration was also investigated, but no clear patterns were identified, meaning that there is not a prevalent component for low or for high concentrations (Figure S7).

3.4 Wildfire episode

A wildfire episode took place from 22 to 26 July 2012 (Figure 7) at 100 km to the NE of MSY, affecting a wide area (Figure S8). It resulted in an average ACSM components + BC concentrations of 16.5 µg m^{-3} over the five-days period. Mainly, the components whose concentrations increased significantly were OA, nitrate and BC, reaching 30-min values of 50 µg m^{-3}, 4.5 µg m^{-3} and 3.6 µg m^{-3}, respectively, which are 9, 8 and 7 times higher than their respective summer averages. The average relative concentration during this episode was dominated by OA (73%).

In order to investigate the wildfire source, an unconstrained source apportionment (PMF) of the organic aerosol fraction during this episode was carried out. The PMF resulted in two factors, one representing the fresh biomass burning organic aerosol (named as BBOA_MSY) and another one interpreted as the mix of other OA sources and aged BBOA, named as OOAm (where the m stands for mix). The interpretation of the factors is based on their mass spectral source profiles and the time series of their contributions. The BBOA_MSY shows higher peaks for the specific tracers of biomass burning (*m/z* 60 and *m/z* 73) (Alfarra et al., 2007) than the OOAm, which indicates that the primary BBOA is well represented by this factor. Moreover, the f44 (ratio of *m/z* 44 (mostly CO_2^+) to total signal in the component mass spectra), an indicator of oxygenated organic species (Alfarra et al., 2007), was higher for the OOAm than for the BBOA_MSY factor, which indicates that this factor corresponds to a more oxidized aerosol. On the other hand, the f43 is higher than the f44 in the BBOA_MSY factor, whereas it is the other way around (f44 much higher than f43) in the OOAm. These differences in relative intensities indicate the differences in the age of the aerosol (Ng et al., 2010) and

Código de campo cambiado
Eliminado: Figure S3
Código de campo cambiado
Eliminado: Figure S4
Eliminado: Figure 7
Eliminado: Figure S5
Eliminado: Aged BBOA
Código de campo cambiado
Eliminado: Aged BB
Código de campo cambiado
Eliminado: Aged
Eliminado: BB
Eliminado: , which led us to identify it as Aged BBOA
Eliminado: Aged BB
Código de campo cambiado

further lead to differentiate the factors as fresh BBOA and OOAm. The SOA formation from biomass burning has been reported to be quick (Heringa et al., 2011), and hence part of the OOAm factor is formed of aged BBOA, which also explains that the time series of the OOAm factor partially tracks that of the BBOA_MSY. The BBOA_MSY profile found here is very similar to a BBOA profile found for Montseny in March 2009 (Minguillón et al., 2011) (https://sites.google.com/site/amsglobaldatabase) and to an average profile for BBOA from various datasets (Ng et al., 2011a) (Figure S9). The f60 in the BBOA_MSY factor is 0.014, similar to the f60 in these other two BBOA profiles (0.017 and 0.024). It has been also compared to the BBOA found in the background of Paris (Crippa et al., 2013), with which some more differences were found, mainly our profile has higher *m/z* 43 and *m/z* 41 signals and lower *m/z* 60 (Figure S9). This BBOA_MSY mass spectrum is considered specific for the study area and hence it can be later used for other studies in the region, to be fed to the ME-2 model in order to quantify the BBOA contribution. We have done so in the present study for the winter period. Whereas the time series of both factors were similar, the BBOA_MSY contribution showed more intense peaks, and the increase in the OOAm was slightly higher for the second part of the main peak on the 23 July.

Eliminado: the
Eliminado: interpretation of
Eliminado: aged BB
Código de campo cambiado
Eliminado: which explains the identification of this factor during the wildfire episode
Código de campo cambiado
Eliminado: Figure S6
Código de campo cambiado
Código de campo cambiado
Con formato: Fuente: Cursiva
Eliminado: Figure S6
Eliminado: Aged BB

3.5 Source apportionment of organic aerosol

The source apportionment of organic aerosol was carried out separately for the warmer period (14 June to 9 October 2012) and the colder period (28 October 2012 to 7 April 2013). The days of the wildfire event were excluded from the warmer period dataset. The separation in two seasons was done to better characterize the source profiles of the different sources, especially the different types of OOA, given that it is expected to vary throughout the year.

The application of ME-2 to the warmer period resulted in a solution with 3 factors: a hydrocarbon-like OA (HOA), a semi-volatile oxygenated OA (SV-OOA) and a low-volatile oxygenated OA (LV-OOA). This solution was chosen based on several tests with different number of factors and different a-values for the constrained factors, taking into account the correlations with external data, the diurnal patterns and the residuals, following the strategy described by Crippa et al. (2014) and Canonaco et al. (2013). The HOA factor was constrained using an average HOA factor (HOA_avg) from different datasets (Ng et al., 2011a). An a-value range from 0.05 to 0.3 was explored and an a-value of 0.2 was finally selected, which was a compromise between a higher Squared Pearson correlation coefficient between HOA and BC (which increased when increasing the a-value) and the physically meaningful profiles of the

Movido (inserción) [2]
Eliminado: Both the number of factors and the a-value
Eliminado: were
Código de campo cambiado
Código de campo cambiado

whole solution (i.e. assessing the profiles of the LV-OOA and SV-OOA factors). BC concentrations correlated moderately with HOA (squared Pearson coefficient R^2= 0.51). The SV-OOA shows higher 43-to-44 ratio compared to the LV-OOA, together with a lower f44, which are the main differences between these two profiles (Figure 8a). The BBOA contribution in summer is expected to be low based on previous studies carried out in July 2009 (Minguillón et al., 2011) and on the low f60 registered in the present study in summer (Figure S10), which is below the background threshold (0.003) established by Cubison et al. (2011). Hence, the BBOA factor was not identified and it was not constrained by the ME-2 in summer.

During the warmer period, the HOA accounted for 13% (0.7 μg m^{-3}), whereas the LV-OOA and the SV-OOA accounted for 45% and 42% of the total OA (2.4 μg m^{-3} and 2.2 μg m^{-3}), respectively (Figure 8c). As explained before, the location and meteorological conditions at MSY result in an increase of pollutants concentrations starting at mid-morning, caused by the breeze transport from populated areas to the regional site. This variation is clearly observed for BC (Figure 9), which showed a moderate correlation with HOA (R^2= 0.51). Nevertheless, the midday increase in the concentration of SV-OOA is larger than that of BC, and therefore it cannot be only explained by the transport of pollutants, including the SOA formed during the transport, but it is attributed to the formation of SOA during these hours in MSY. Hence, the SOA formation can be estimated as the additional increase with respect to that of BC (considered in % of the average concentration during the night hours), which results in a local SOA formation of 1.1 μg m^{-3}. This SOA may result mainly from biogenic precursors, in agreement with the 70% of non-fossil SOA found in March 2009 (Minguillón et al., 2011). The flatter diurnal pattern of LV-OOA (Figure 9) points to a more regional and well-oxidized aerosol, which could be interpreted as the regional background SOA. This SOA formation during warm periods was also observed by Cusack et al. (2013), who studied nucleation and particle growth events, identifying both of them even under polluted conditions at MSY.

In the colder period, the application of ME-2 resulted in a solution with 3 factors: hydrocarbon-like OA (HOA), biomass burning OA (BBOA) and oxygenated OA (OOA) (Figure 8b). A solution with two OOA factors was investigated and it was not meaningfully interpretable. Probably the small temperature range variation in winter results in not enough diurnal variation in f43 and f44 for a split of the OOA in SV-OOA and LV-OOA. As per the warmer period, the final solution was chosen based on the strategy described by Crippa et al. (2014) and Canonaco et al. (2013). The residuals for the chosen solution did not show any daily pattern or *m/z*-dependent pattern, which is a good indicator that the selected solution explains the OA variation. For coherence with the warmer period, the HOA factor was based in an average HOA factor (HOA_avg) from different datasets (Ng et al., 2011a), and it was

Eliminado: higher

Subido [2]: Both the number of factors and the a-value were chosen based on several tests with different number of factors and different a-values for the constrained factors, taking into account the correlations with external data, the diurnal patterns and the residuals, following the strategy described by Crippa et al. (2014) and Canonaco et al. (2013).

Eliminado: Figure 8

Código de campo cambiado

Eliminado: Figure S7

Código de campo cambiado

Eliminado: Figure 8

Eliminado: with the breeze

Eliminado: Figure 9

Eliminado: . BC concentrations correlate

Eliminado: ly

Eliminado: squared Pearson coefficient

Código de campo cambiado

Eliminado: Figure 9

Código de campo cambiado

Eliminado: Figure 8

Movido (inserción) [1]

Con formato: Fuente: Cursiva

Eliminado: T

Código de campo cambiado

constrained with an a-value of 0.1. This a-value was chosen based on the correlation between the HOA contribution and the BC concentrations found for different a-values tests. The HOA contribution shows a relatively strong correlation with BC concentrations (squared Pearson coefficient R^2=0.70). The HOA spectral profiles found for summer and winter are quite similar, and hence the HOA contributions in summer and winter can be compared directly. The BBOA factor was decided to be constrained based on the f60 signal, which was above the aforementioned threshold of 0.003 (Figure S10). It was based in the BBOA_MSY profile found for the wildfire episode that took place during this study, constrained with an a-value of 0.1. The a-value was chosen with the following criteria: preference for a low a-value given that the anchor profile used was site-specific, residuals for the *m/z* 60 not showing any diurnal pattern, contribution of the BBOA factor to the total *m/z* 60 (which reached 64% for the chosen solution). The resulting BBOA profile has a higher *m/z* 44 signal than the BBOA_MSY, which may indicate differences in the biomass burning emissions from the wildfire event compared to the emissions from regular biomass burning, or it could indicate that the BBOA contribution identified here may be partially mixed with some oxidized OA. The single winter OOA factor identified shows higher f44 than both LV-OOA and SV-OOA in summer. This higher degree of oxidation of the OA in winter indicates that there is less newly-formed SOA during winter compared to summer. A similar variation was observed in Zurich (Canonaco et al., 2014). The OOA contribution correlates moderately with sulphate (R^2=0.49), relatively strongly with nitrate (R^2=0.73) and more strongly with ammonium (R^2=0.79).

The major OA constituent in winter was the OOA, with 59% (1.5 µg m^{-3}), whereas the HOA and BBOA accounted for 12% (0.3 µg m^{-3}) and 29% (0.7 µg m^{-3}) of the total OA, respectively (Figure 8d). Note that the BBOA contribution may be mixed with some OOA as stated before, given the relatively high signal at *m/z* 44 and hence the pure BBOA contribution would be lower than that determined. Actually it accounts for 6% of the total signal at *m/z* 44. Nevertheless, strong correlation (R^2=0.77) was found between the BBOA contribution and the potassium concentrations determined in 24-h PM_1 samples (Figure S11), which further confirms the existence of this source at MSY in winter. The relative BBOA contributions found in the present study are similar to those found in a previous study in March 2009 using a HR-ToF-AMS, where the HOA represented 7% of the total OA, the BBOA contributed with 9% and the rest was attributed to OOA (Minguillón et al., 2011;Crippa et al., 2014). The discrepancy in the BBOA contribution (29% vs 9%) may be due to the different sampling periods (the current study included Nov 2012-March 2013 whereas the previous study only included March 2009), to the mixture of some OOA in the BBOA factor for the present study, and/or to the possible increase of biomass burning due to the climate and energy policies in the last five years.

Eliminado:

Eliminado: Figure S7

Con formato: Fuente: Cursiva

Eliminado: Only one OOA was identified for the colder period.

Subido [1]: A solution with two OOA factors was investigated and it was not meaningfully interpretable. Probably the small temperature range variation in winter results in not enough diurnal variation in f43 and f44 for a split of the OOA in SV-OOA and LV-OOA.

Código de campo cambiado

Eliminado: Figure 8

Con formato: Fuente: Cursiva

Eliminado: 64

Código de campo cambiado

Código de campo cambiado

The average daily pattern shown by the different OA sources in winter (Figure 9) resembles that of BC, nitrate, sulphate and ammonium (Figure 5), with an increase of pollutants concentrations starting at around 10h UTC and reaching high concentrations at around 13h UTC. This daily increase is attributed to the transport from populated areas to the mountain site with the breeze. This variation is observed for all the components and therefore the local formation of SOA is deduced to be low in winter.

Eliminado: Figure 9

Eliminado: Figure 5

4 CONCLUSIONS

The deployment of an ACSM at the regional background site of Montseny during one year allowed for the characterization of PM_1 composition and its variation as a function of time of the year and atmospheric scenarios. The OA sources were also identified and studied.

Strong correlation (R^2=0.66) was found between total mass determined by ACSM components + BC and PM_1 determined by an optical particle counter with a slope near to unity. The suitability of the application of a composition-dependent collection efficiency (CE) was confirmed.

Strong correlations were found between the ACSM measurements and off-line measurements (filters) for sulphate (R^2=0.93), ammonium (R^2=0.68) and nitrate (R^2=0.82). Nevertheless the slopes differ more than 20% from the unity for nitrate and ammonium.

The comparison of the OA measured by the ACSM with the OC measured in filter samples points to a current underestimation of the RIE established for OA.

A wildfire episode affected significantly the organic aerosol concentrations. The source profile of fresh BBOA for this specific episode was characterized and it resembles those from other studies.

OA was the major component of submicron aerosol on average and especially during the warm periods. Three organic sources were identified by PMF in summer: HOA, SV-OOA and LV-OOA; and three sources in winter: HOA, BBOA and OOA. SOA was the major constituent of the OA at MSY, being more than 85% of total OA in summer and about 60% in winter. The in-situ formation of SOA in summer, happening around midday, was estimated to be 1.1 µg m^{-3} on average (20% of OA).

Sulphate concentrations were higher in summer, while nitrate concentrations were higher in winter due to environmental conditions (temperature, relative humidity and solar radiation, among others). Sulphate originates from a wider area and is affected by the shipping emissions from the Mediterranean, while the rest of the components may have a nearer origin.

As typical for mountain sites, all the pollutants were affected by the general breeze regime, leading to an increase from mid-morning until the afternoon, and a decrease until the evening.

ACKNOWLEDGEMENTS

This study was supported by the Spanish Ministry of Economy and Competitiveness and FEDER funds under the project PRISMA (CGL2012-39623-C02-1), by the Generalitat de Catalunya (AGAUR 2015 SGR33 and the DGQA), and by the European Union Seventh Framework Programme (FP7/ 2007-2013) through ACTRIS (grant agreement no 262254). M.C. Minguillón was partially funded by the JAE-Doc CSIC program, co-funded by the European Social Fund (ESF). A. Ripoll was partially funded by a PhD grant from the Spanish Ministry of Economy and Competitiveness through CARIATI (CGL2008-06294/CLI) project.

Eliminado: 2009 SGR8

FIGURE CAPTIONS

Figure 1. ACSM components + BC concentrations vs PM_1 measured by the optical counter coloured by the sampling time (dd/mm/aaaa). Line and parameters correspond to least orthogonal distance fit (y=a+bx). The wild fire period is excluded from the fit.

Figure 2. ACSM components concentrations vs 24-h samples concentrations. Lines and parameters correspond to least orthogonal distance fits.

Figure 3. Time series of ACSM components and BC concentrations during the whole study period.

Figure 4. Monthly relative chemical composition of submicron aerosol. The numbers on top of each bar represent the average monthly concentration. n is the number of data points for each month (right axis).

Figure 5. Average daily pattern for (a) the warmer and (b) the colder periods. Note that OA is plotted in the right axis.

Figure 6. Relative chemical composition of submicron aerosol as a function of the type of scenario. The numbers on top of each bar represent the average concentration for each type of scenario. n is the number of data points for each type of scenario (right axis).

Figure 7. (a) Time series of ACSM components and BC concentrations and pie chart of the average chemical composition during the wildfire episode from 22nd to 26th July 2012. (b) Time series of the contribution of the BBOA_MSY and Aged BBOA sources identified by PMF. (c) Source profile of the BBOA_MSY and Aged BBOA sources.

Figure 8. Mass spectral profiles of the organic sources identified for (a) summer and (b) winter. Average contribution of the organic sources to total OA for (c) summer and (d) winter.

Figure 9. Average daily patterns of the organic sources contributions and BC concentrations for (a) summer and (b) winter. Error bars represent standard deviations.

SUPPLEMENTARY MATERIAL

Figure S1. Frequency of type of scenario for each of the months of the study period.

Figure S2. Temperature, relative humidity, wind direction and speed, solar radiation and precipitation hourly data at MSY during the study period.

Figure S3. Time-dependent CE calculated with the Middlebrook approach (Middlebrook et al., 2012).

Figure S4. ACSM components + BC concentrations vs mass concentration calculated from Scanning Mobility Particle Sizer (SMPS) data coloured by the sampling time (dd/mm/aaaa). Data availability for SMPS data covered only 2012 period. Line and parameters correspond to least orthogonal distance fit (y=a+bx). The wild fire period is excluded from the fit.

Figure S5. Schematic comparison of ACSM components + BC concentrations vs PM_1 concentrations from OPC corrected with gravimetric determinations. The numbers indicate the slopes found for experimental data for Montseny during June 2012 to July 2013. The 2.25 corresponds to the slope of OA (ACSM) vs OM estimated from OC (filters) as 2*OC.

Figure S6. Average daily pattern for (a) Atlantic advections (ATL), (b) North African episodes (NAF), (c) regional episodes (REG), and (d) Winter Anticyclonic episodes (WAE). Note that OA is plotted in the right axis.

Figure S7. Relative chemical composition as a function of average concentration and number of data points for each range of concentrations. No clear differences are observed.

Figure S8. Total optical depth, sulfate surface concentration, dust surface concentration, and smoke surface concentration from the NAAPS model for 23, 24 and 25 July 2012 (wildfire event) (a-c), and satellite images from 22 and 23 July 2012 from The Earth Observing System Data and Information System (EOSDIS), NASA's Earth Science Data Systems Program (d, e).

Figure S9. Comparison of the BBOA factor found for the wildfire episode (BBOA_MSY) with other BBOA profiles found in the literature (Ng et al., 2011a;Crippa et al., 2014).

Figure S10. Time series of f60 (unitless) and OA concentration (μg m^{-3}) throughout the study period at MSY. Dashed line corresponds to the 0.5% threshold for the f60 determined by Cubison et al. (2011).

Figure S11. Contribution of BBOA in winter (averaged to 24-h periods matching the filter sampling) vs potassium concentrations in PM_1.

Eliminado: 3

Eliminado: 4

Eliminado: 5

Eliminado: 6

Código de campo cambiado

Código de campo cambiado

Eliminado: 7

Código de campo cambiado

REFERENCES

Aiken, A. C., Decarlo, P. F., Kroll, J. H., Worsnop, D. R., Huffman, J. A., Docherty, K. S., Ulbrich, I. M., Mohr, C., Kimmel, J. R., Sueper, D., Sun, Y., Zhang, Q., Trimborn, A., Northway, M., Ziemann, P. J., Canagaratna, M. R., Onasch, T. B., Alfarra, M. R., Prevot, A. S. H., Dommen, J., Duplissy, J., Metzger, A., Baltensperger, U., and Jimenez, J. L.: O/C and OM/OC ratios of primary, secondary, and ambient organic aerosols with high-resolution time-of-flight aerosol mass spectrometry, Environ. Sci. Technol., 42, 4478-4485, 2008.

Alastuey, A., Minguillón, M. C., Pérez, N., Querol, X., Viana, M., and de Leeuw, F.: PM10 measurement methods and correction factors: 2009 status report, ETC/ACM Technical Paper 2011/21, 2011.

Alfarra, M. R., Prevot, A. S. H., Szidat, S., Sandradewi, J., Weimer, S., Lanz, V. A., Schreiber, D., Mohr, M., and Baltensperger, U.: Identification of the mass spectral signature of organic aerosols from wood burning emissions, Environ. Sci. Technol., 41, 5770-5777, 2007.

723 Alves, C., Vicente, A., Pio, C., Kiss, G., Hoffer, A., Decesari, S., Prevôt, A. S. H.,
724 Minguillón, M. C., Querol, X., Hillamo, R., Spindler, G., and Swietlicki, E.: Organic compounds in
725 aerosols from selected European sites - Biogenic versus anthropogenic sources, Atmos.
726 Environ., 59, 243-255, 2012.

727 Bougiatioti, A., Stavroulas, I., Kostenidou, E., Zarmpas, P., Theodosi, C., Kouvarakis, G.,
728 Canonaco, F., Prévôt, A. S. H., Nenes, A., Pandis, S. N., and Mihalopoulos, N.: Processing of
729 biomass-burning aerosol in the eastern Mediterranean during summertime, Atmos. Chem.
730 Phys., 14, 4793-4807, 2014.

731 Budisulistiorini, S. H., Canagaratna, M. R., Croteau, P. L., Marth, W. J., Baumann, K.,
732 Edgerton, E. S., Shaw, S. L., Knipping, E. M., Worsnop, D. R., Jayne, J. T., Gold, A., and Surratt, J.
733 D.: Real-time continuous characterization of secondary organic aerosol derived from isoprene
734 epoxydiols in downtown Atlanta, Georgia, using the aerodyne aerosol chemical speciation
735 monitor, Environ. Sci. Technol., 47, 5686-5694, 2013.

736 Budisulistiorini, S. H., Canagaratna, M. R., Croteau, P. L., Baumann, K., Edgerton, E. S.,
737 Kollman, M. S., Ng, N. L., Verma, V., Shaw, S. L., Knipping, E. M., Worsnop, D. R., Jayne, J. T.,
738 Weber, R. J., and Surratt, J. D.: Intercomparison of an Aerosol Chemical Speciation Monitor
739 (ACSM) with ambient fine aerosol measurements in downtown Atlanta, Georgia, Atmos. Meas.
740 Tech., 7, 1929-1941, 10.5194/amt-7-1929-2014, 2014.

741 Canagaratna, M. R., Jayne, J. T., Jimenez, J. L., Allan, J. D., Alfarra, M. R., Zhang, Q.,
742 Onasch, T. B., Drewnick, F., Coe, H., Middlebrook, A., Delia, A., Williams, L. R., Trimborn, A. M.,
743 Northway, M. J., DeCarlo, P. F., Kolb, C. E., Davidovits, P., and Worsnop, D. R.: Chemical and
744 microphysical characterization of ambient aerosols with the aerodyne aerosol mass
745 spectrometer, Mass Spectrom. Rev., 26, 185-222, 2007.

746 Canonaco, F., Crippa, M., Slowik, J. G., Baltensperger, U., and Prévôt, A. S. H.: SoFi, an
747 IGOR-based interface for the efficient use of the generalized multilinear engine (ME-2) for the
748 source apportionment: ME-2 application to aerosol mass spectrometer data, Atmospheric
749 Measurement Techniques, 6, 3649-3661, 2013.

750 Canonaco, F., Slowik, J. G., Baltensperger, U., and Prévôt, A. S. H.: Inverse relationship
751 between the degree of oxidation of OOA (oxygenated organic aerosol) and the oxidant OX (O3
752 +NO2) due to biogenic emissions, Atmos. Chem. Phys. Discuss., 14, 28079-28104,
753 10.5194/acpd-14-28079-2014, 2014.

754 Carbone, S., Saarikoski, S., Frey, A., Reyes, F., Reyes, P., Castillo, M., Gramsch, E., Oyola,
755 P., Jayne, J., Worsnop, D., and Hillamo, R.: Chemical characterization of submicron Aerosol
756 particles in Santiago de Chile, Aerosol and Air Quality Research, 13, 462-473, 2013.

757 Cavalli, F., Viana, M., Yttri, K. E., Genberg, J., and Putaud, J. P.: Toward a standardised
758 thermal-optical protocol for measuring atmospheric organic and elemental carbon: the
759 EUSAAR protocol, Atmos. Meas. Tech., 3, 79-89, 10.5194/amt-3-79-2010, 2010.

760 Crippa, M., DeCarlo, P. F., Slowik, J. G., Mohr, C., Heringa, M. F., Chirico, R., Poulain, L.,
761 Freutel, F., Sciare, J., Cozic, J., Di Marco, C. F., Elsasser, M., Nicolas, J. B., Marchand, N., Abidi,
762 E., Wiedensohler, A., Drewnick, F., Schneider, J., Borrmann, S., Nemitz, E., Zimmermann, R.,
763 Jaffrezo, J. L., Prévôt, A. S. H., and Baltensperger, U.: Wintertime aerosol chemical composition
764 and source apportionment of the organic fraction in the metropolitan area of Paris, Atmos.
765 Chem. Phys., 13, 961-981, 10.5194/acp-13-961-2013, 2013.

766 Crippa, M., Canonaco, F., Lanz, V. A., Äijälä, M., Allan, J. D., Carbone, S., Capes, G.,
767 Ceburnis, D., Dall'Osto, M., Day, D. A., DeCarlo, P. F., Ehn, M., Eriksson, A., Freney, E., Ruiz, L.
768 H., Hillamo, R., Jimenez, J. L., Junninen, H., Kiendler-Scharr, A., Kortelainen, A. M., Kulmala, M.,
769 Laaksonen, A., Mensah, A. A., Mohr, C., Nemitz, E., O'Dowd, C., Ovadnevaite, J., Pandis, S. N.,
770 Petäjä, T., Poulain, L., Saarikoski, S., Sellegri, K., Swietlicki, E., Tiitta, P., Worsnop, D. R.,
771 Baltensperger, U., and Prévôt, A. S. H.: Organic aerosol components derived from 25 AMS data
772 sets across Europe using a consistent ME-2 based source apportionment approach, Atmos.
773 Chem. Phys., 14, 6159-6176, 2014.

774 Cubison, M. J., Ortega, A. M., Hayes, P. L., Farmer, D. K., Day, D., Lechner, M. J., Brune,
775 W. H., Apel, E., Diskin, G. S., Fisher, J. A., Fuelberg, H. E., Hecobian, A., Knapp, D. J., Mikoviny,
776 T., Riemer, D., Sachse, G. W., Sessions, W., Weber, R. J., Weinheimer, A. J., Wisthaler, A., and
777 Jimenez, J. L.: Effects of aging on organic aerosol from open biomass burning smoke in aircraft
778 and laboratory studies, Atmos. Chem. Phys., 11, 12049-12064, 2011.

779 Cusack, M., Alastuey, A., Pérez, N., Pey, J., and Querol, X.: Trends of particulate matter
780 (PM2.5) and chemical composition at a regional background site in the Western
781 Mediterranean over the last nine years (2002–2010), Atmos. Chem. Phys., 12, 8341-8357,
782 10.5194/acp-12-8341-2012, 2012.

783 Cusack, M., Pérez, N., Pey, J., Wiedensohler, A., Alastuey, A., and Querol, X.: Variability
784 of sub-micrometer particle number size distributions and concentrations in the Western
785 Mediterranean regional background, Tellus, Series B: Chemical and Physical Meteorology, 65,
786 2013.

787 Fröhlich, R., Crenn, V., Setyan, A., Belis, C. A., Canonaco, F., Favez, O., Riffault, V.,
788 Slowik, J. G., Aas, W., Aijälä, M., Alastuey, A., Artiñano, B., Bonnaire, N., Bozzetti, C., Bressi, M.,
789 Carbone, C., Coz, E., Croteau, P. L., Cubison, M. J., Esser-Gietl, J. K., Green, D. C., Gros, V.,
790 Heikkinen, L., Herrmann, H., Jayne, J. T., Lunder, C. R., Minguillón, M. C., Močnik, G., O'Dowd,
791 C. D., Ovadnevaite, J., Petralia, E., Poulain, L., Priestman, M., Ripoll, A., Sarda-Estève, R.,
792 Wiedensohler, A., Baltensperger, U., Sciare, J., and Prévôt, A. S. H.: ACTRIS ACSM
793 intercomparison – Part 2: Intercomparison of ME-2 organic source apportionment results from
794 15 individual, co-located aerosol mass spectrometers, Atmos. Meas. Tech. Discuss., 8, 1559-
795 1613, 10.5194/amtd-8-1559-2015, 2015.

796 Hawkins, L. N., Russell, L. M., Covert, D. S., Quinn, P. K., and Bates, T. S.: Carboxylic
797 acids, sulfates, and organosulfates in processed continental organic aerosol over the southeast
798 Pacific Ocean during VOCALS-REx 2008, Journal of Geophysical Research: Atmospheres, 115,
799 10.1029/2009jd013276, 2010.

800 Heringa, M. F., DeCarlo, P. F., Chirico, R., Tritscher, T., Dommen, J., Weingartner, E.,
801 Richter, R., Wehrle, G., Prévôt, A. S. H., and Baltensperger, U.: Investigations of primary and
802 secondary particulate matter of different wood combustion appliances with a high-resolution
803 time-of-flight aerosol mass spectrometer, Atmos. Chem. Phys., 11, 5945-5957, 2011.

804 IPCC: Climate Change 2013: The Physical Science Basis. Contribution of Working Group
805 I to the Fifth Assessment Report of the Intergovernmental Panel on Climate Change, edited by:
806 Stocker, T. F., Qin, D., Plattner, G.-K., Tignor, M., Allen, S. K., Boschung, J., Nauels, A., Xia, Y.,
807 Bex, V., and Midgley, P. M., Cambridge University Press, Cambridge, United Kingdom and New
808 York, NY, USA, 1535 pp pp., 2013.

809 Jimenez, J. L., Canagaratna, M. R., Donahue, N. M., Prevot, A. S. H., Zhang, Q., Kroll, J.
810 H., DeCarlo, P. F., Allan, J. D., Coe, H., Ng, N. L., Aiken, A. C., Docherty, K. S., Ulbrich, I. M.,
811 Grieshop, A. P., Robinson, A. L., Duplissy, J., Smith, J. D., Wilson, K. R., Lanz, V. A., Hueglin, C.,
812 Sun, Y. L., Tian, J., Laaksonen, A., Raatikainen, T., Rautiainen, J., Vaattovaara, P., Ehn, M.,
813 Kulmala, M., Tomlinson, J. M., Collins, D. R., Cubison, M. J., Dunlea, E. J., Huffman, J. A.,
814 Onasch, T. B., Alfarra, M. R., Williams, P. I., Bower, K., Kondo, Y., Schneider, J., Drewnick, F.,
815 Borrmann, S., Weimer, S., Demerjian, K., Salcedo, D., Cottrell, L., Griffin, R., Takami, A.,
816 Miyoshi, T., Hatakeyama, S., Shimono, A., Sun, J. Y., Zhang, Y. M., Dzepina, K., Kimmel, J. R.,
817 Sueper, D., Jayne, J. T., Herndon, S. C., Trimborn, A. M., Williams, L. R., Wood, E. C.,
818 Middlebrook, A. M., Kolb, C. E., Baltensperger, U., and Worsnop, D. R.: Evolution of organic
819 aerosols in the atmosphere, Science, 326, 1525-1529, 2009.

820 Liu, P. S. K., Deng, R., Smith, K. A., Williams, L. R., Jayne, J. T., Canagaratna, M. R.,
821 Moore, K., Onasch, T. B., Worsnop, D. R., and Deshler, T.: Transmission efficiency of an
822 aerodynamic focusing lens system: Comparison of model calculations and laboratory
823 measurements for the aerodyne aerosol mass spectrometer, Aerosol Sci. Technol., 41, 721-
824 733, 2007.

825 Middlebrook, A. M., Bahreini, R., Jimenez, J. L., and Canagaratna, M. R.: Evaluation of
826 composition-dependent collection efficiencies for the Aerodyne aerosol mass spectrometer
827 using field data, Aerosol Sci. Technol., 46, 258-271, 2012.

828 Millán, M. M., Salvador, R., Mantilla, E., and Kallos, G.: Photooxidant dynamics in the
829 Mediterranean basin in summer: Results from European research projects, Journal of
830 Geophysical Research D: Atmospheres, 102, 8811-8823, 1997.

831 Minguillón, M. C., Perron, N., Querol, X., Szidat, S., Fahrni, S. M., Alastuey, A., Jimenez,
832 J. L., Mohr, C., Ortega, A. M., Day, D. A., Lanz, V. A., Wacker, L., Reche, C., Cusack, M., Amato,
833 F., Kiss, G., Hoffer, A., Decesari, S., Moretti, F., Hillamo, R., Teinilä, K., Seco, R., Peñuelas, J.,
834 Metzger, A., Schallhart, S., Müller, M., Hansel, A., Burkhart, J. F., Baltensperger, U., and Prévôt,
835 A. S. H.: Fossil versus contemporary sources of fine elemental and organic carbonaceous
836 particulate matter during the DAURE campaign in Northeast Spain, Atmos. Chem. Phys., 11,
837 12067-12084, 10.5194/acp-11-12067-2011, 2011.

838 Ng, N. L., Canagaratna, M. R., Zhang, Q., Jimenez, J. L., Tian, J., Ulbrich, I. M., Kroll, J. H.,
839 Docherty, K. S., Chhabra, P. S., Bahreini, R., Murphy, S. M., Seinfeld, J. H., Hildebrandt, L.,
840 Donahue, N. M., DeCarlo, P. F., Lanz, V. A., Prévôt, A. S. H., Dinar, E., Rudich, Y., and Worsnop,
841 D. R.: Organic aerosol components observed in Northern Hemispheric datasets from Aerosol
842 Mass Spectrometry, Atmos. Chem. Phys., 10, 4625-4641, 10.5194/acp-10-4625-2010, 2010.

843 Ng, N. L., Canagaratna, M. R., Jimenez, J. L., Zhang, Q., Ulbrich, I. M., and Worsnop, D.
844 R.: Real-time methods for estimating organic component mass concentrations from aerosol
845 mass spectrometer data, Environ. Sci. Technol., 45, 910-916, 2011a.

846 Ng, N. L., Herndon, S. C., Trimborn, A., Canagaratna, M. R., Croteau, P. L., Onasch, T. B.,
847 Sueper, D., Worsnop, D. R., Zhang, Q., Sun, Y. L., and Jayne, J. T.: An Aerosol Chemical
848 Speciation Monitor (ACSM) for routine monitoring of the composition and mass
849 concentrations of ambient aerosol, Aerosol Sci. Technol., 45, 770-784, 2011b.

850 Paatero, P., and Tapper, U.: Positive matrix factorization: a non-negative factor model
851 with optimal utilization of error estimates of data values, Environmetrics, 5, 111-126, 1994.

852 Paatero, P.: The multilinear engine - a table-driven, least squares program for solving
853 multilinear problems, including the n-way parallel factor analysis model, Journal of
854 Computational and Graphical Statistics, 8, 854-888, 1999.

855 Pérez, N., Pey, J., Castillo, S., Viana, M., Alastuey, A., and Querol, X.: Interpretation of
856 the variability of levels of regional background aerosols in the Western Mediterranean, Sci.
857 Total Environ., 407, 527-540, 2008.

858 Petit, J. E., Favez, O., Sciare, J., Crenn, V., Sarda-Estève, R., Bonnaire, N., Močnik, G.,
859 Dupont, J. C., Haeffelin, M., and Leoz-Garziandia, E.: Two years of near real-time chemical
860 composition of submicron aerosols in the region of Paris using an Aerosol Chemical Speciation
861 Monitor (ACSm) and a multi-wavelength Aethalometer, Atmos. Chem. Phys. Discuss., 14,
862 24221-24271, 10.5194/acpd-14-24221-2014, 2014.

863 Petzold, A., Ogren, J. A., Fiebig, M., Laj, P., Li, S. M., Baltensperger, U., Holzer-Popp, T.,
864 Kinne, S., Pappalardo, G., Sugimoto, N., Wehrli, C., Wiedensohler, A., and Zhang, X. Y.:
865 Recommendations for reporting black carbon measurements, Atmos. Chem. Phys., 13, 8365-
866 8379, 2013.

867 Pey, J., Pérez, N., Castillo, S., Viana, M., Moreno, T., Pandolfi, M., López-Sebastián, J.
868 M., Alastuey, A., and Querol, X.: Geochemistry of regional background aerosols in the Western
869 Mediterranean, Atmospheric Research, 94, 422-435, 2009.

870 Pey, J., Pérez, N., Querol, X., Alastuey, A., Cusack, M., and Reche, C.: Intense winter
871 atmospheric pollution episodes affecting the Western Mediterranean, Sci. Total Environ., 408,
872 1951-1959, 2010.

873 Pope III, C. A., and Dockery, D. W.: Health effects of fine particulate air pollution: Lines
874 that connect, Journal of the Air and Waste Management Association, 56, 709-742, 2006.

875 Querol, X., Alastuey, A., Pey, J., Cusack, M., Pérez, N., Mihalopoulos, N., Theodosi, C.,
876 Gerasopoulos, E., Kubilay, N., and Koçak, M.: Variability in regional background aerosols within
877 the Mediterranean, Atmos. Chem. Phys., 9, 4575-4591, 2009.

878 Querol, X., Alastuey, A., Viana, M., Moreno, T., Reche, C., Minguillón, M. C., Ripoll, A.,
879 Pandolfi, M., Amato, F., Karanasiou, A., Pérez, N., Pey, J., Cusack, M., Vázquez, R., Plana, F.,
880 Dall'Osto, M., De La Rosa, J., Sánchez De La Campa, A., Fernández-Camacho, R., Rodríguez, S.,
881 Pio, C., Alados-Arboledas, L., Titos, G., Artíñano, B., Salvador, P., García Dos Santos, S., and
882 Fernández Patier, R.: Variability of carbonaceous aerosols in remote, rural, urban and industrial
883 environments in Spain: Implications for air quality policy, Atmos. Chem. Phys., 13, 6185-6206,
884 2013.

885 Querol, X., Alastuey, A., Pandolfi, M., Reche, C., Pérez, N., Minguillón, M. C., Moreno,
886 T., Viana, M., Escudero, M., Orio, A., Pallarés, M., and Reina, F.: 2001-2012 trends on air quality
887 in Spain, Sci. Total Environ., 490, 957-969, 2014.

888 Ripoll, A., Minguillón, M. C., Pey, J., Jimenez, J. L., Day, D. A., Querol, X., and Alastuey,
889 A.: Long-term real-time chemical characterization of submicron aerosols at Montsec (Southern
890 Pyrenees, 1570 m a.s.l.), Atmos. Chem. Phys. Discuss., 14, 28809-28844, 10.5194/acpd-14-
891 28809-2014, 2014a.

892 Ripoll, A., Minguillón, M. C., Pey, J., Pérez, N., Querol, X., and Alastuey, A.: Joint
893 analysis of continental and regional background environments in the Western Mediterranean:

Con formato: Español (alfab. internacional)

894 PM1 and PM10 concentrations and composition, Atmos. Chem. Phys. Discuss., 14, 16001-
895 16041, 10.5194/acpd-14-16001-2014, 2014b.

896 Shaw, S. L., Baumann, K., Budisulistiorini, S., Canagaratna, M., Croteau, P., Edgerton, E.,
897 Jansen, J., Jayne, J., Knipping, E., Marth, W., Mueller, S., Ng, S., Surratt, J., Tanner, R., and
898 Weber, R.: Operation of the aerosol chemical speciation monitor (ACSM) in the southeastern
899 U.S, 2012, 110-114,

900 Sun, Y., Wang, Z., Dong, H., Yang, T., Li, J., Pan, X., Chen, P., and Jayne, J. T.:
901 Characterization of summer organic and inorganic aerosols in Beijing, China with an Aerosol
902 Chemical Speciation Monitor, Atmos. Environ., 51, 250-259, 2012.

903 Sun, Y., Wang, Z., Fu, P., Jiang, Q., Yang, T., Li, J., and Ge, X.: The impact of relative
904 humidity on aerosol composition and evolution processes during wintertime in Beijing, China,
905 Atmos. Environ., 77, 927-934, 2013a.

906 Sun, Y. L., Wang, Z. F., Fu, P. Q., Yang, T., Jiang, Q., Dong, H. B., Li, J., and Jia, J. J.:
907 Aerosol composition, sources and processes during wintertime in Beijing, China, Atmos. Chem.
908 Phys., 13, 4577-4592, 2013b.

909 Takahama, S., Johnson, A., Guzman Morales, J., Russell, L. M., Duran, R., Rodriguez, G.,
910 Zheng, J., Zhang, R., Toom-Sauntry, D., and Leaitch, W. R.: Submicron organic aerosol in
911 Tijuana, Mexico, from local and Southern California sources during the CalMex campaign,
912 Atmos. Environ., 70, 500-512, 2013.

913 Van Drooge, B. L., Cusack, M., Reche, C., Mohr, C., Alastuey, A., Querol, X., Prevot, A. S.
914 H., Day, D. A., Jimenez, J. L., and Grimalt, J. O.: Molecular marker characterization of the
915 organic composition of submicron aerosols from Mediterranean urban and rural environments
916 under contrasting meteorological conditions, Atmos. Environ., 61, 482-489, 2012.

917 Wiedensohler, A., Birmili, W., Nowak, A., Sonntag, A., Weinhold, K., Merkel, M.,
918 Wehner, B., Tuch, T., Pfeifer, S., Fiebig, M., Fjäraa, A. M., Asmi, E., Sellegri, K., Depuy, R.,
919 Venzac, H., Villani, P., Laj, P., Aalto, P., Ogren, J. A., Swietlicki, E., Williams, P., Roldin, P.,
920 Quincey, P., Hüglin, C., Fierz-Schmidhauser, R., Gysel, M., Weingartner, E., Riccobono, F.,
921 Santos, S., Grüning, C., Faloon, K., Beddows, D., Harrison, R., Monahan, C., Jennings, S. G.,
922 O'Dowd, C. D., Marinoni, A., Horn, H. G., Keck, L., Jiang, J., Scheckman, J., McMurry, P. H.,
923 Deng, Z., Zhao, C. S., Moerman, M., Henzing, B., De Leeuw, G., Löschau, G., and Bastian, S.:
924 Mobility particle size spectrometers: Harmonization of technical standards and data structure
925 to facilitate high quality long-term observations of atmospheric particle number size
926 distributions, Atmospheric Measurement Techniques, 5, 657-685, 2012.
927
928
929

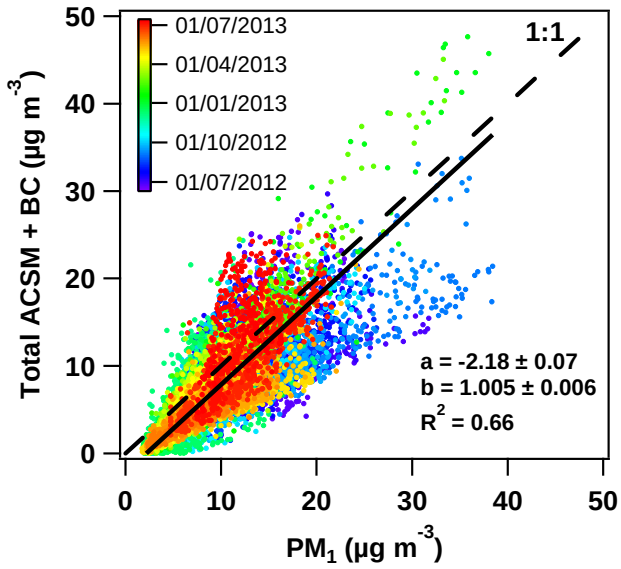

930

931 **Figure 1**

932

933

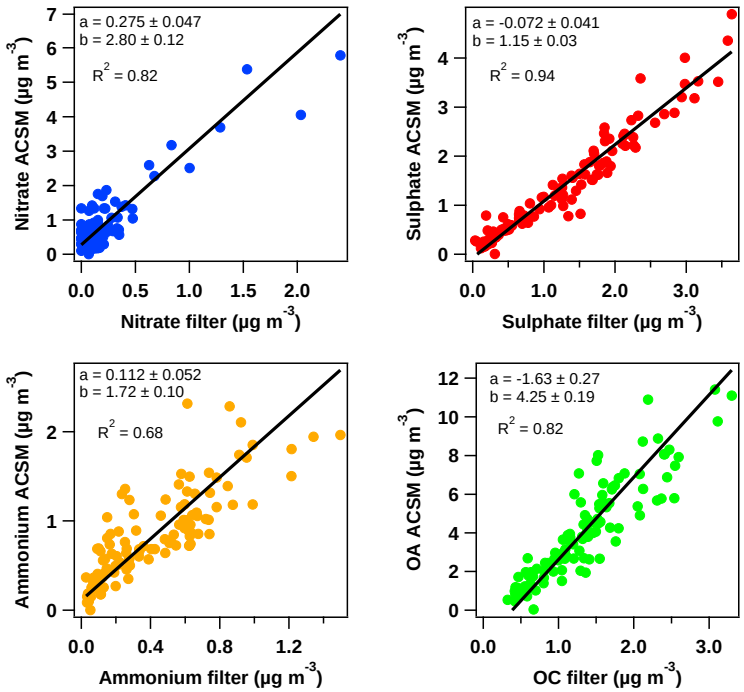

934

935

936

937 **Figure 2**

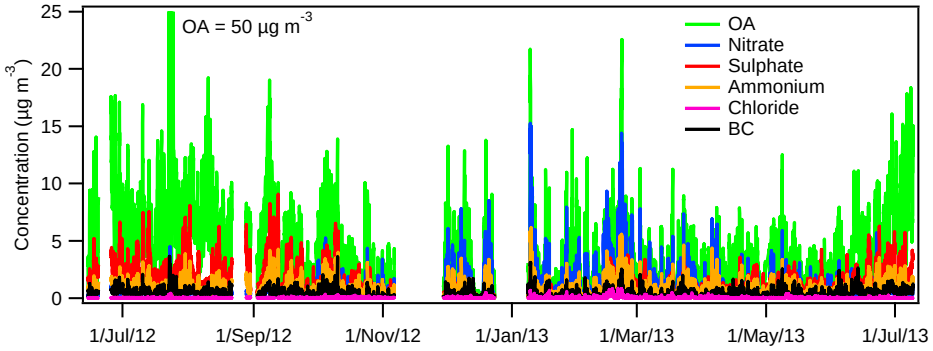

Figure 3

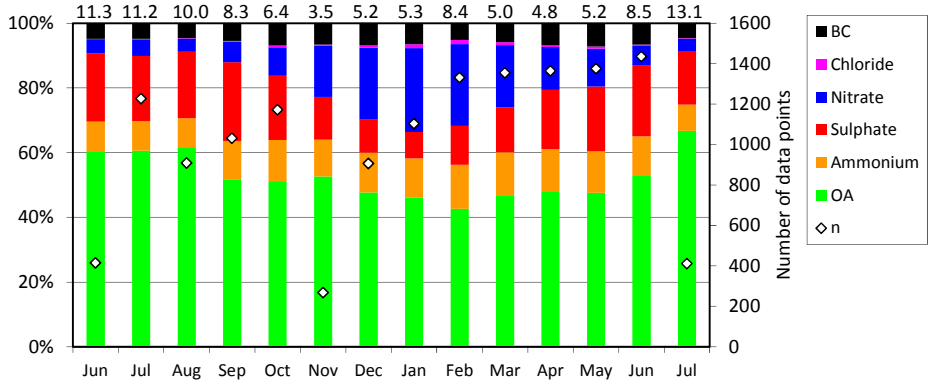

Figure 4

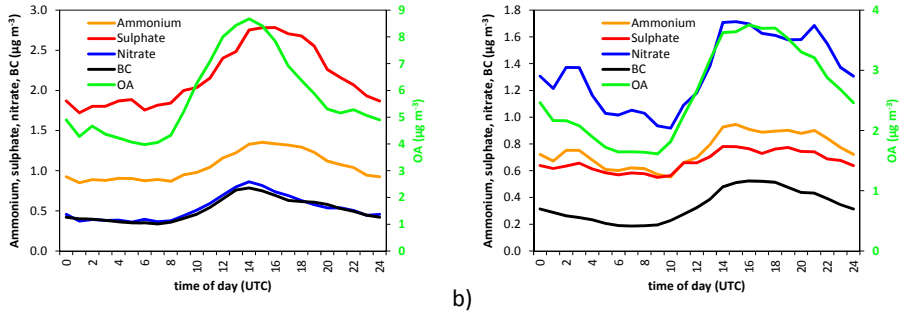

951 a) b)

952 **Figure 5**

953

954

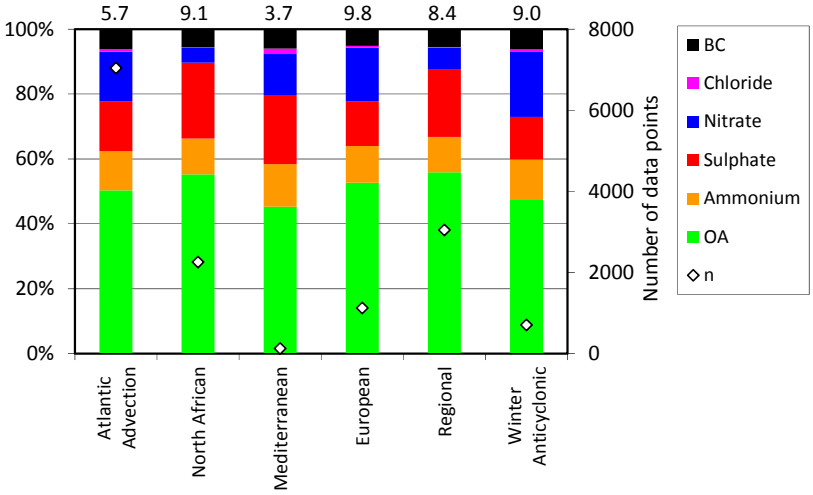

955

956 **Figure 6**

957

958

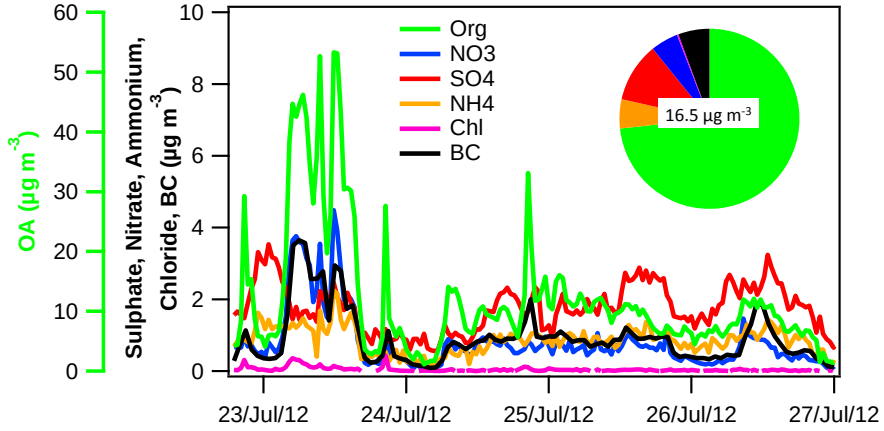
OA (µg m-3)
Sulphate, Nitrate, Ammonium, Chloride, BC (µg m-3)
Org
NO3
SO4
NH4
Chl
BC
16.5 µg m-3
23/Jul/12
24/Jul/12
25/Jul/12
26/Jul/12
27/Jul/12

a)

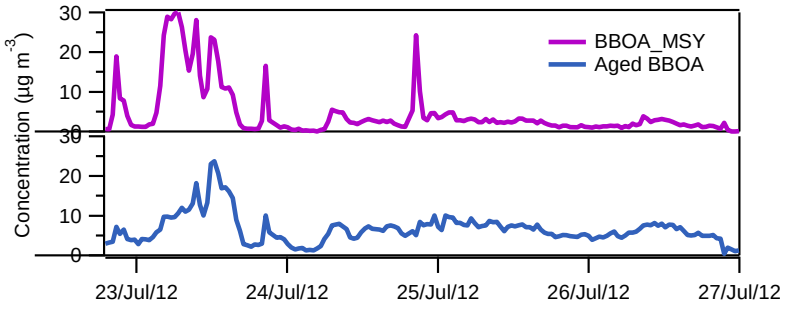
Concentration (µg m-3)
BBOA_MSY
Aged BBOA
23/Jul/12
24/Jul/12
25/Jul/12
26/Jul/12
27/Jul/12

b)

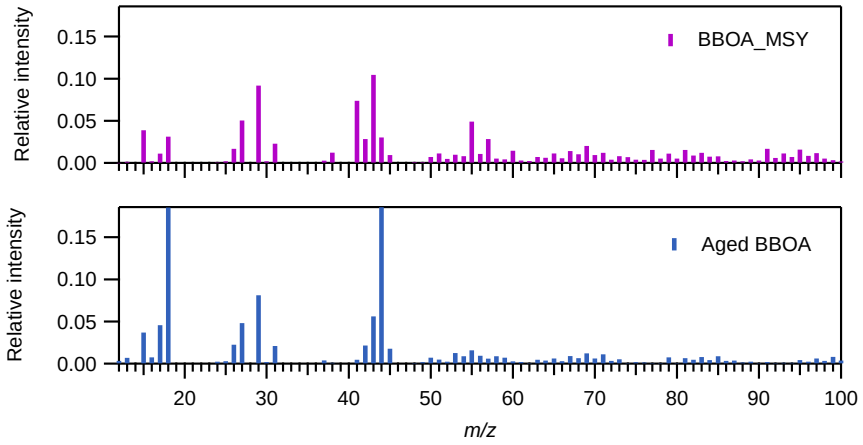
Relative intensity
BBOA_MSY
Aged BBOA
m/z

c)

Figure 7

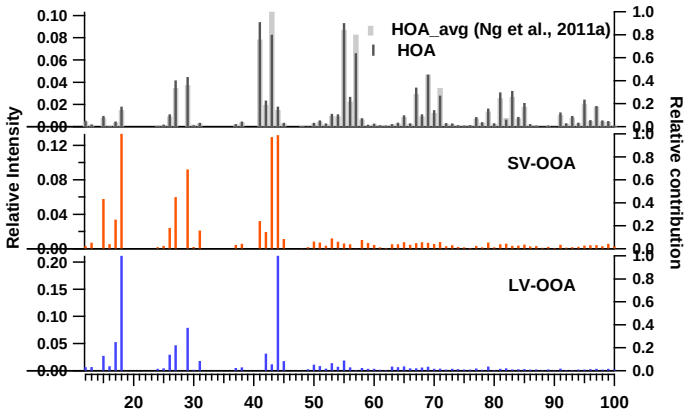

968 a)

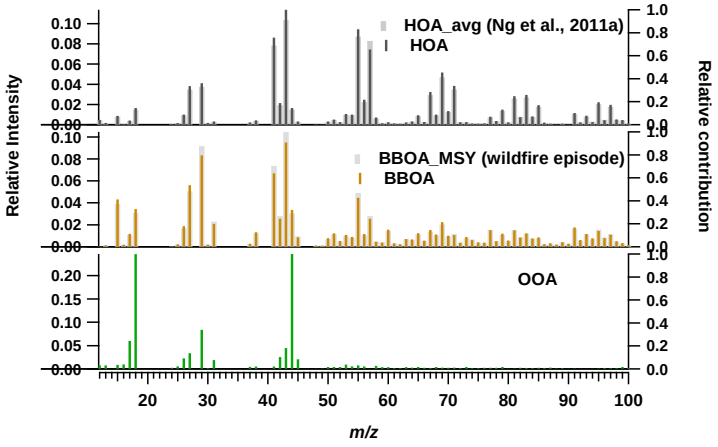

969 b)

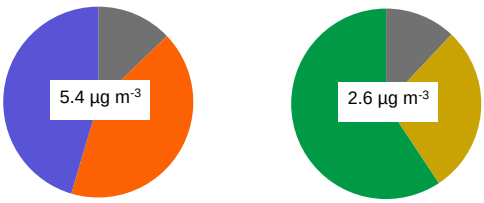

970 c) d)

971

972 **Figure 8**

973

974

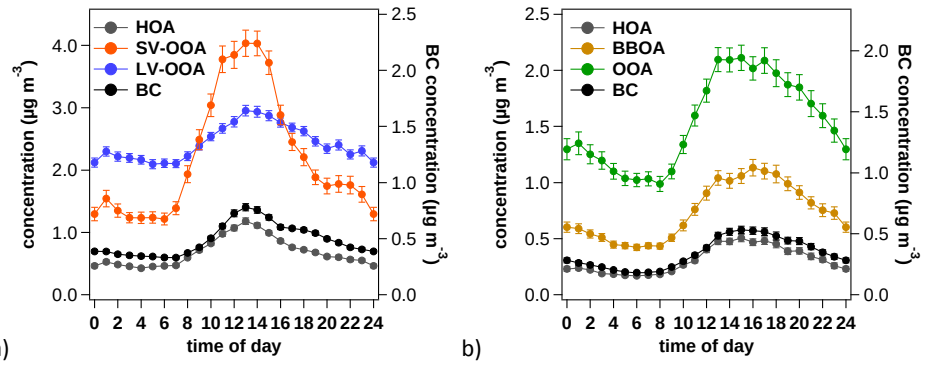
HOA
SV-OOA
LV-OOA
BC
concentration (µg m-3)
BC concentration (µg m-3)
time of day
a)
HOA
BBOA
OOA
BC
concentration (µg m-3)
BC concentration (µg m-3)
time of day
b)

Figure 9